NATIONAL ADVISORY COMMITTEE FOR AERONAUTICS

TECHNICAL MEMORANDUM

No. 1121

THEORETICAL INVESTIGATION OF DRAG REDUCTION IN MAINTAINING THE LAMINAR BOUNDARY LAYER BY SUCTION

By A. Ulrich

Translation

"Theoretische Untersuchungen über die Widerstandsersparnis durch Laminarhaltung mit Absaugung"

Aerodynamisches Institut der Technischen Hochschule Braunschweig
Bericht Nr. 44/8

Washington
June 1947

NATIONAL ADVISORY COMMITTEE FOR AERONAUTICS

TECHNICAL MEMORANDUM NO. 1121

THEORETICAL INVESTIGATION OF DRAG REDUCTION BY MAINTAINING THE LAMINAR BOUNDARY LAYER BY SUCTION*

By A. Ulrich

ABSTRACT

Maintenance of a laminar boundary layer by suction was suggested recently to decrease the friction drag of an immersed body, in particular an airfoil section [1]. The present treatise makes a theoretical contribution to this question in which, for several cases of suction and blowing, the stability of the laminar velocity profile is investigated. Estimates of the minimum suction quantities for maintaining the laminar boundary layer and estimates of drag reduction are thereby obtained.

OUTLINE

*"Theoretische Untersuchungen über die Widerstandsersparnis durch Laminarhaltung mit Absaugung." Aerodynamisches Institut der Technischen Hochschule Braunschweig, Bericht Nr. 44/8, March 20, 1944.

I. STATEMENT OF THE PROBLEM

Recent investigations established the fact that the drag on a wing may be reduced by maintaining a laminar boundary layer. The first method to obtain a large region of laminar flow is to select a profile which has the minimum pressure position as far back as possible. Suction of the boundary layer as indicated by Betz [1] is another means to move the transition point from laminar to turbulent flow as far back as possible. The present investigation makes a theoretical contribution to the problem of transition laminar/turbulent in the boundary layer under suction and blowing conditions. To this end an examination of the stability of the laminar boundary layer with suction was made.

Suction always has a stabilizing effect on the laminar layer, that is, the transition point is moved downstream; whereas blowing has destabilizing effect. The stabilizing effect of the suction results from: first, a reduction of the boundary layer thickness (a thin boundary layer is less inclined to become turbulent than a thicker one, other conditions being equal); and second, changes in the shape of the laminar velocity distribution and therefore: an increase in the critical Reynolds number of the boundary layer $(U\delta^*/\nu)_{crit}$ (U = velocity outside the boundary layer, δ^* = displacement thickness, see chapter II, ν = kinematic viscosity). In both cases there is an analogy to the influence of a negative pressure gradient on the boundary layer.

Theoretical calculation of the transition laminar/turbulent must be based on knowledge of the laminar velocity distribution and requires considerable accuracy. H. Schlichting and K. Bussmann [3] and R. Iglisch [4] gave exact solutions of the boundary layer with suction and blowing and these solutions are suitable for an examination of stability. The following cases were investigated:

(1) The boundary layer on the flat plate in longitudinal flow with suction and blowing distributed according to $v_o(x) \sim 1/\sqrt{x}$ (x = distance along the plate.)

(2) The boundary layer on the flat plate in longitudinal flow with uniform suction, v_o = const., starting at the front edge of the plate.

(3) The boundary-layer for a flat plate with an impinging jet with uniform suction or uniform blowing.

Only the results of an investigation of the stability of a laminar boundary layer on a flat plate in longitudinal flow and with uniform suction are at present available. For this case, the thickness of the boundary layer is constant at a large distance from the leading edge of the plate:

$$\delta^* = \frac{\nu}{-v_o} \tag{1}$$

The velocity distribution of this asymptotic suction profile is dependent on y only, and is, according to H. Schlichting [5], as follows:

$$\frac{U(y)}{U_o} = 1 - e^{-\frac{y}{\delta^*}}; \quad v(x,y) = v_o = \text{const.} \tag{2}$$

The critical Reynolds number for this asymptotic suction profile is according to K. Bussmann and H. Münz [2] $(U_o\delta^*/\nu)_{crit}$ = 70,000. Since for the plate in longitudinal flow without suction $(U_o\delta^*/\nu)_{crit}$ = 575, the suction in this case increases the critical Reynolds number by a factor of about 100.

From the known Reynolds number with suction, the minimum suction quantity necessary for maintaining the laminar boundary layer can be determined immediately (since $\delta^* \leq \delta^*_{crit}$)

$$\frac{U_o\delta^*}{\nu} = \frac{U_o}{-v_o}\,\frac{-v_o\delta^*}{\nu} \leq \left(\frac{U_o\delta^*}{\nu}\right)_{crit}$$

Then from equation (1) $-v_o\delta^*/\nu = 1$, the minimum suction quantity is:

$$c_{Q\ crit} = \frac{-v_o}{U_o} \geq \frac{1}{70,000} = 0.14 \times 10^{-4} \qquad (3)$$

Since the quantity is small the maintenance of a laminar boundary layer by suction seems rather promising; therefore further investigations of the stability for the boundary layer with suction were carried out in this report. The minimum suction quantity for maintaining the laminar boundary layer and the drag reduction shall be established.

II. SYMBOLS

x, y	rectangular coordinates parallel and perpendicular to the wall; $x = y = 0$ at the leading edge of the plate, or the stagnation point (figs. 1, 4, and 7)
l	length of plate
b	width of plate
$U(x)$	potential flow outside of the boundary layer; $U = u_1x$ for the plane stagnation flow $U = U_o$ for the flat plate in longitudinal flow
U_o	free-stream velocity
u, v	components of velocity in the boundary layer parallel and perpendicular to the wall, respectively

$v_0(x)$	prescribed normal velocity at the wall; $v_0 > 0$ blowing, $v_0 < 0$ suction
τ_0	shear stress at the wall
$\delta^* = \int_0^\infty \left(1 - \frac{u}{U}\right) dy$	displacement thickness of the boundary layer
$\vartheta = \int_0^\infty \frac{u}{U}\left(1 - \frac{u}{U}\right) dy$	momentum thickness of the boundary layer
Q	total suction quantity and blowing quantity, respectively, for the plate in longitudinal flow; $Q < 0$ suction, $Q > 0$ blowing
$c_Q = \frac{-Q}{lb \times U_0}$	nondimensional quantity rate of flow coefficient for the flat plate; for the plate with uniform suction this coefficient becomes $c_Q = \frac{-v_0}{U_0}$ $(v_0 = \text{const});$ $c_Q > 0$ suction, $c_Q < 0$ blowing
$C = c_Q\sqrt{\frac{U_0 l}{\nu}}$	reduced flow coefficient for the flat plate with the suction distributed as $v_0(x) \sim 1/\sqrt{x}$
$\xi = \left(\frac{-v_0}{U_0}\right)^2 \frac{U_0 x}{\nu} = c_Q^2 \times \frac{U_0 x}{\nu}$	nondimensional extent of laminar flow for the plate flow with uniform suction
$C_0 = \frac{-v_0}{\sqrt{u_1 \nu}}$	reduced flow coefficient for the plane stagnation flow
$c_f = \frac{W_R}{b\, l\, \frac{\rho}{2} U_0^2}$	friction drag coefficient for the flat plate in longitudinal flow (plate wetted on one side)

III. EXAMINATION OF THE STABILITY OF LAMINAR VELOCITY PROFILES

(a) Flat plate with suction and blowing according to $v_o \approx 1/\sqrt{x}$.

The first series of the investigated velocity profiles concerns the flat plate in longitudinal flow with continuous suction where the suction velocity is distributed according to $v_o \sim 1/\sqrt{x}$ (fig. 1). Schlichting and Bussmann [3] gave exact solutions of the differential equations for the boundary layer with suction and blowing for this case. It is a characteristic of this case that each velocity profile along the plate is related to a prescribed mass flow coefficient. The reduced flow coefficient

$$C = c_Q\sqrt{Re} = c_Q\sqrt{U_o l/\nu}$$

appears decisive. Herein

$$c_Q = - Q/l\ b\ U_o$$

stands for the ordinary flow coefficient for the plate of the length l and the width b, and $Re = U_o l/\nu$ for the Reynolds number of the plate. Positive flow coefficients correspond to suction, negative ones to blowing. For this case all the blowing profiles have a point of inflection.

The velocity profiles for the flow coefficients $C = -\frac{1}{4}; \frac{1}{2}; 1$ and $\frac{3}{2}$, that is, one blowing profile with a point of inflection and three suction profiles were selected for the investigations of stability. These profiles together with the profile for $C = 0$ (flat plate without suction) are given in terms of y/δ^* in figure 2. The second derivatives of these velocity distributions, which are essential for the calculation of stability, are drawn in figure 3. Table 5 shows the connection between δ^* and the region of the laminar flow x.

(b) Flat plate with uniform suction: v_o = const.

The second series of velocity profiles along the plate are for the case of uniform suction (v_o = constant) these profiles were calculated exactly by Iglisch [4]. Figure 4 shows the flow along the flat plate with uniform suction which was investigated by Iglisch, and figure 5 represents the examined velocity profiles. The velocity profiles with increasing

$$\xi = \left(\frac{-v_o}{U_o}\right)^2 \frac{U_o x}{\nu} = c_Q^2 \frac{U_o x}{\nu} \tag{4}$$

starting at the form of the Blasius profile at $\xi = 0$, gradually approach the asymptotic suction profile according to equation (2) [5]. The second derivatives of these velocity profiles are drawn in figure 6. All the velocity profiles have negative curvature throughout ($\partial^2u/\partial y^2 < 0$). With increasing ξ the absolute values of $\partial^2u/\partial y^2$ increase rapidly. Figure 7 and table 7 represent the nondimensional parameters of the boundary layer, namely the displacement thickness $-v_o\delta^*/\nu$, momentum thickness $\frac{-v_o\vartheta}{\nu}$ shear stress $\tau_o\delta^*/\mu U_o$ and shape parameter δ^*/ϑ as functions of $\sqrt{\xi}$ according to Iglisch's calculations [4]. Six profiles with the parameters ξ = 0.005; 0.02; 0.08; 0.18; 0.32 and 0.5 were examined with respect to stability. The results for $\xi = 0$ and $\xi = \infty$ are known from [2].

(c) Flat plate with an impinging jet with uniform suction.

As a third series several stagnation point profiles from those calculated exactly by Schlichting and Bussmann [3] were examined with respect to stability. The potential flow is in this case (compare fig. 7)

$$U(x) = u_1 x; \quad V(y) = -u_1 y$$

Figure 8 shows this plane stagnation flow. Figure 9 shows the velocity profiles which were investigated. Their shape changes with the flow coefficient

$$C_o = \frac{-v_o}{\sqrt{u_1 \nu}} \tag{5}$$

Positive values of C_o correspond to suction and negative values of C_o to blowing. The profile with $C_o = 0$ is Hiemenz' profile of the boundary layer; this profile results from the first term in the power series starting at the stagnation point for the boundary layer of the circular cylinder.

The velocity profiles with the flow coefficients $C_o = -3.1905$; -1.198; 0; 0.5; 1.095 and 1.9265, that is, two blowing profiles, the profile with an impermeable wall $C_o = 0$ and three suction profiles were selected for the stability investigations. Figure 10 shows the second derivatives of these velocity profiles which have negative values throughout. Table 7 shows the corresponding boundary-layer parameters.

IV. STABILITY CALCULATIONS

The examination of stability for these laminar velocity profiles was carried out according to the method of small vibrations in the same way as previously given in detail by W. Tollmien [10] and H. Schlichting [6]. A plane disturbance motion in the form of a wave motion progressing in the direction of the flow is superimposed over the basic flow. It is essential that the basic flow U(y) be assumed dependent on the coordinate y only. Then the amplitude distribution of the basic flow also is a function of y only. The equation

$$\left(u' = \frac{\delta\psi}{\delta y}, \ v' = -\frac{\delta\psi}{\delta x}\right.$$

$$\psi(x,y) = \varphi(y)\, e^{i\alpha(x - ct)} \tag{6}$$

is valid for the flow function $\psi(x,y)$ of the superimposed disturbance motion (u', v'). α is real and gives the wave length λ of the disturbance motion, $\lambda = 2\pi/\alpha$. $c = c_r + ic_i$ is complex; c_r represents the wave velocity of transmission and c_i, positive or negative, the excitation or damping, respectively. $\varphi(y) = \varphi_r(y) + i\varphi_i(y)$ gives the complex amplitude function. The ordinary linear differential equation of the fourth order

$$(U - c)\ (\varphi'' - \alpha^2\varphi) - U''\varphi = \frac{-i}{\alpha R}\ (\varphi'''' - 2\alpha^2\varphi'' + \alpha^4\varphi) \quad (7)$$

with the boundary conditions

$$y = 0:\ \varphi = \varphi' = 0;\ y = \infty:\ \varphi = \varphi' = 0 \qquad (8)$$

is obtained for that function from Navier-Stokes' equations. In equation (7) all values are rendered nondimensional with a suitable boundary-layer thickness δ and the potential velocity U. $R = U\delta/\nu$ stands for the Reynolds number; ' signifies differentiation with respect to y/δ. The boundary-layer conditions result from the disappearance of the normal and tangential components of the disturbance velocity at the wall and outside of the boundary-layer $(y = \infty)$. The examination of stability of the prescribed basic flow $U(y)$ is a characteristic value problem of that differential equation in the following sense, since $U(y)$ the wave length $\lambda = 2\pi/\alpha$ and the Reynolds number $U\delta/\nu$ are prescribed. The complex characteristic value $c = c_r + ic_i$ is required for every two corresponding values α, R; from the real part of c results the velocity of transmission of the superimposed disturbance; the imaginary part of c is decisive for the stability. Disturbance occurring for the condition of neutral stability $(c_i = 0)$ are especially interesting, and lie on a curve (neutral stability curve) in the α, R plane. The neutral stability curve separates the stable disturbances from the unstable ones. (See figs. 14 to 16.) The tangent to the neutral stability curve parallel to the α-axis gives the smallest Reynolds number at which a neutrally stable disturbance is still possible. This number is the critical Re-number of the basic flow.

In examining the stability of the suction profiles, the boundary conditions of equation (8) were held the same as in the case of the impermeable wall; that is, disappearance of the normal and tangential disturbance velocities at the wall is required for the boundary layer with suction also, although the normal component of the basic flow at the wall is different from zero.

The numerical solution of the characteristic value problem then takes exactly the same course as indicated by W. Tollmien [10] and H. Schlichting [6] and needs, therefore, no further explanation here. For the stability calculation, the velocity profiles are approximated by parabolas in the form:

$$\frac{u}{U} = 1 - p\ (a - y/\delta)^n \tag{9}$$

with

$$\delta = 3\delta^*$$

The constants p, a, and n for the three investigated series of profiles are enumerated in table 1. The closest agreement with the exact velocity profiles near the wall was important. (Figs. 2, 5, and 8.) The polar diagrams for the examined velocity profiles are given in figures 11 to 13 as an intermediate result of the stability calculation. The neutral stability curves were obtained from these diagrams and $\alpha\delta^*$ is plotted against $U_0\delta^*/\nu$ in figures 14 to 16 and corresponding values are tabulated in tables 2 to 4. These curves show that the stability is greatly increased by suction while blowing decreases it.

Figure 14 shows in detail that in the plate flow with continuous suction the neutral stability curves for positive flow coefficients C lie between those for the flat plate without suction and those for the asymptotic suction profile, which were calculated previously by Bussmann and Münz [2]. The case of blowing with $C = -\frac{1}{4}$ demonstrates clearly the enlargement of the region of instability.

As to the flow along the plate, figure 15 shows that the neutral stability curves for the values of ξ used here also lie between the curves for $\xi = 0$ (flat plate without suction) and $\xi = \infty$ (asymptotic suction profile). For increasing ξ the region of instability diminishes and at $\xi = 0.5$ the neutral stability curve appears to approach the curve of the asymptotic suction profile.

The stability in the stagnation flow also is greatly increased by suction; with increasing flow coefficient C_0 the neutral stability curves (fig. 16) approach the curve of the asymptotic suction profile for the flat plate. It is of interest that the neutral stability curves for the investigated cases of blowing still lie inside the curve for the impermeable flat plate.

The critical Reynolds number $(U_0\delta^*/\nu)_{crit}$ is the tangent parallel to the ordinate of the neutral stability curves. The critical Reynolds numbers for the three series of stability examinations are enumerated in table 5.

The following detailed result was obtained for the plate flow with continuous suction $(v_0 \sim 1/\sqrt{x})$: $(U_0\delta^*/\nu)_{crit} = 204$ for the blowing profile $\left(C = -\frac{1}{4}\right)$ and therefore is far below the critical Reynolds number 575 for the impermeable flat plate. With suction the Reynolds number increases rapidly and reaches for $C = \frac{3}{2}$ the value of 19,100, thus evidently approaching the critical Reynolds number 70,000 for the asymptotic suction profile determined by Bussmann-Münz [2]. Figure 17 shows how the transition point on the plate is shifted backward with increasing suction. The Reynolds numbers formed by the displacement thickness are, for different flow coefficients C, plotted against the Re numbers formed from the distance (x) measured along the plate in this figure 17 and also figure 18, and values are tabulated in table 5. The stability limit of the impermeable wall $(U_0x/\nu)_{crit} = 1.1 \times 10^5$; but for a flow coefficient $C = 1$ critical Re exceeds 10^7

and therefore reaches the Re-number region of today's large and fast airplanes.[1] Figure 19 shows the dependency of the critical Reynolds number on the shape parameter δ^*/θ.

Flow along the <u>plate with uniform suction</u> (v_o = const.), the critical Reynolds-numbers for different $\sqrt{\xi}$ compiled in table 5 lie between the critical Reynolds numbers 575 for the impermeable wall and 70000 for the asymptotic suction profile. Figure 20 shows the result of the stability calculation in which the critical Reynolds numbers $(U_o\delta^*/\upsilon)_{crit}$ are represented as functions of the nondimensional flow distance $\sqrt{\xi}$. In figure 21 the onset of instability is ascertained. Here both the stability limit $(U_o\delta^*/\upsilon)_{crit}$ according to figure 20 and the nondimensional boundary-layer thickness $U_o\delta^*/\upsilon$ plotted against $\sqrt{\xi}$ for different flow coefficients $c_Q = -v_o/U_o$ are shown. The boundary-layer thickness is obtained from

$$\frac{U_o\delta^*}{\upsilon} = \frac{-v_o\delta^*}{\upsilon}\,\frac{U_o}{-v_o} \tag{10}$$

the values of $-v_o\delta^*/\upsilon$ as functions of $\sqrt{\xi}$ are given in figure 7. Since for $\xi\rightarrow\infty$: $-v_o\delta^*/\upsilon = 1$, the separate curves have the asymptotes

$$\xi = \infty: \quad \left(\frac{U_o\delta^*}{\upsilon}\right)_\infty = \frac{U_o}{-v_o} \tag{11}$$

The point of transition is given by the intersection of a curve $U_o\delta^*/\upsilon$ with the stability limit $(U_o\delta^*/\upsilon)_{crit}$.

---

[1] C = 1 means $c_Q\sqrt{\frac{U_o l}{\upsilon}} = 1$, that is, with $U_o l/\upsilon = 10^7$. $c_Q = 3.16 \times 10^{-4}$.

The onset of instability occurs before $\sqrt{\xi} = 0.1$ for the flow coefficients $-\frac{v_o}{U_o} = \frac{1}{70,000}, \frac{1}{20,000}, \frac{1}{10,000}$; on the other hand, there is no intersection for $-\frac{v_o}{U_o} > \frac{1}{8500}$.

Flow coefficients

$$\boxed{c_{Q_{crit}} \geq \frac{1}{8500} = 1.18 \times 10^{-4}} \tag{12}$$

are, therefore, sufficient for maintaining the laminar boundary layer for the entire preliminary laminar flow region. This value is to be compared with the value $c_{Q_{crit}} = \frac{1}{70,000} = 0.14 \times 10^{-4}$ determined by Bussmann and Munz (reference 2) for the asympototic suction profile. The minimum flow coefficient necessary for maintaining the laminar boundary layer is, therefore, increased by about the factor 10, if the preliminary laminar flow region is taken into consideration. The earlier investigation had already led to this presumption. The minimum suction quantity[2] found herewith is $c_{Q_{crit}} = 1.18 \times 10^{-4}$;

---

[2]One could consider the possibility of reducing the total suction quantity still further than $c_{Q_{crit}} = 1/8500$. One would have to select such a distribution of $-v_o(x)$ as to make the curve $U_o\delta^*/\nu$ in figure 20 remain everywhere just underneath the stability limit $(U_o\delta^*/\nu)_{crit}$. The necessary distribution $[-v_o(x)/U_o]_{crit}$ is given to a first approximation by the intersections of the curves $U_o\delta^*/\nu$ for different $-v_o/U_o$ with the stability limit (fig. 21). One then obtains up to about $\sqrt{\xi} = 0.1$ an increasing local flow coefficient $[-v_o(x)/U_o]_{crit}$; the maximum is reached with 1/8500 at about $\sqrt{\xi} = 0.1$; for higher $\sqrt{\xi}$ there is again a decrease down to the constant asymptote $(-v_o/U_o)_\infty = 1/70000$. The total suction quantity, however, would hardly be reduced under the constant value $c_{Q_{crit}} = 1/8500$ for practical purposes if such an "optimum" nonuniform distribution of suction were selected: For a plate with the Reynolds number $U_o l/\nu = 10^7$ and

this quantity is still so small that the maintaining of the laminar boundary layer by suction appears quite promising. We mention, for comparison with experimental results, that the necessary suction quantities in Holstein's [7] measurements on the supporting wing are $c_Q = 1.1 \times 10^{-4}$ to 2.8×10^{-4}. This value is, however, not exactly comparable to the thoeretical one since the suction in the measurements was produced through slots.

Figure 19 represents the critical Re-number $(U_0\delta^*/\nu)_{crit}$ as a function of the shape parameter δ^*/ϑ. Simultaneously, the results of the stability calculation for the velocity profiles of the flat plate with continuous suction $v_0 \sim 1/\sqrt{x}$ are drawn into this diagram. One can see that the critical Reynolds numbers of the two stability calculations lie on the same curve. Hence it is concluded that the critical Reynolds number $(U_0\delta^*/\nu)_{crit}$ is dependent on the shape parameter δ^*/ϑ only.

Plane stagnation flow.- The critical Reynolds number $(U_0\delta^*/\nu)_{crit}$ for the impermeable wall $(C_0 = 0)$ is 12,300; for the suction quantity $(C_0 = 1.9265)$ this figure increases to 38,000 (fig. 22). With blowing the critical Reynolds number decreases slowly; the value of 707 is reached at $C_0 = -3.1905$ (table 5). These critical Reynolds numbers also are given as functions of δ^*/ϑ in figure 19; one can see that they take a course similar to the flow along the plate although they lie somewhat underneath this curve.

$-v_0/U_0 = 10^{-4}$, $\sqrt{\xi_1} = \left(\frac{-v_0}{U_0}\right)\sqrt{\frac{U_0 l}{\nu}} = -0.3$; therefore the region where c_Q can be considerably smaller than 1/8500 is still far beyond the end of the plate.

V. APPLICATION OF THE RESULTS TO DRAG REDUCTION BY MAINTAINING THE LAMINAR BOUNDARY LAYER

The drag coefficient c_f is plotted against the Reynolds number in figure 23 for the laminar and turbulent flow in the boundary layer of the flat plate with continuous suction $v_0 \sim 1/\sqrt{x}$. The drag-coefficient curves from reference [3] for different quantities of suction and blowing C also are shown in the figure [3] in this diagram; the coefficients c_f increase with increasing suction quantities.[3] Drag may be reduced by suction in the region between the curve for the laminar flow of the flat plate $(C = 0)$ and the fully turbulent curve, if the laminar boundary layer can be maintained there by suction. The result of the stability calculation given in figure 18, that is, the critical Reynolds number $(U_0x/\nu)_{crit}$ as a function of the mass coefficient C, was transferred to this diagram and yields the curve denoted "stability limit." This curve signifies that for conditions (C, Re) above this limit the suction quantity is sufficient to maintain the laminar boundary layer at the respective Reynolds number.

The drag reduction by maintaining the laminar boundary layer for different Reynolds numbers can be specified immediately by means of this diagram. The minimum suction quantity $c_{Q\ crit} = C_{crit}/\sqrt{Re}$ necessary for maintaining the laminar boundary layer is determined for a given Reynolds number; then the drag coefficient c_f for the fully turbulent and laminar flow with suction is read off the ordinate. This calculation is carried out for the most interesting Reynolds numbers from 2×10^6 to 10^8 in table 6. One can see that for instance for $Re \doteq 10^7$ a drag reduction of more than 70 percent can be obtained. This statement, however, does not yet make allowance for the power required

---

[3] The frictional drag coefficients represent in the present case of continuous suction the total drag, because there is no additional sink drag of the suction quantity since the parts sucked off spent their x-impulse fully in the boundary layer already. Compare Schlichting [8].

for the suction blower. But this power is not excessive, since only very small suction quantities are needed here.

Figure 23 was concerned with the plate flow with continuous suction; in a similar way, in figure 24 the laminar frictional drag coefficient c_f (determined according to Iglisch's [4] calculations) for the plate flow with uniform suction is plotted against the Reynolds number $U_0 l/\nu$ with the flow coefficient $c_Q = -v_0/U_0$ as parameter. For very small Reynolds numbers, all curves converge to the curve of the plate without suction. c_f becomes contant with the value $c_{f\infty} = -2v_0/U_0$ for high Reynolds numbers where the larger part of the plate lies within the region of the asymptotic solution with constant boundary layer. The curve

$c_{Q\ crit} = \dfrac{-v_0}{U_0} = 1.18 \times 10^{-4}$, named "stability limit"

was drawn into the diagram (fig. 24) as the result of the stability calculation. Figure 25 represents the same condition again; but, different from figure 24, c_f is given on the ordinate in ordinary scale. Both representations show that for instance at $Re = 10^7$ a drag reduction of 80 percent of the fully turbulent frictional drag can be achieved. Figure 26 compares the drag reductions by maintaining the laminar boundary layer and the critical suction quantities for the two cases uniform suction and $v_0 \sim 1/\sqrt{x}$.

A comparison of the results obtained under the assumption of uniform suction v_0 = constant with the results based on the suction rule $v_0 \sim 1/\sqrt{x}$ demonstrates the following: The critical suction quantity $c_{Q\ crit}$ for continuous suction $v_0 \sim 1/\sqrt{x}$ is variable with $Re = U_0 l/\nu$ and is for all $Re < 7 \times 10^7$ larger than the suction quantity for uniform suction which is constant $c_{q\ crit} = 1.18 \times 10^{-4}$. The drag reduction for uniform suction also is larger in the considered region of Reynolds numbers than for $v_0 \sim 1/\sqrt{x}$; for instance, the drag reduction at $Re = 10^7$ is 80 percent against 73 percent. Therefore, the uniform suction is at any rate preferable to the suction with $v_0 \sim 1/\sqrt{x}$ for the whole region $5 \times 10^6 < Re < 10^8$ that is, the main region of interest for practical purposes.

At high Re-numbers (over 10^8) only the suction according to the rule $v_o(x) \sim 1/\sqrt{x}$ shows smaller critical suction quantities and higher drag reduction than uniform suction. Table 6 and figure 26 give a comparison of the critical suction quantities and the drag reductions for the two suction rules.

VI. MEASUREMENTS OF THE VELOCITY DISTRIBUTION IN THE LAMINAR BOUNDARY LAYER WITH SUCTION

Finally, a few results of experiments about the boundary layer with suction shall be given. In figure 27 two measured velocity distributions with the asymptotic suction profile [5] and the Blasius profile for the plane plate in longitudinal flow without suction are compared. The first measurement was carried out by Holstein [7] on a wing with the profile NACA 0012-64; the measurement was taken at $x/l = 0.9$ (l = wing chord) of the wing center section on the suction side ($\alpha = 0^o$), with six suction slots of the suction side opened. The velocity distribution which was converted into the displacement thickness conforms rather well with the asymptotic suction profile of the flat plate with uniform suction while differing greatly from the Blasius profile with impermeable wall.

The second measurement was taken by Ackeret [9] ; a suction channel with numerous narrow slots a short distance behind the suction length was used. This velocity distribution also takes a course similar to the asymptotic suction profile. Therefore, the few existing measurements show good agreement with the theory as to the form of laminar velocity distribution with and without suction, respectively.

VII. SUMMARY

Stability calculations were carried out on three series of exactly calculated velocity profiles for the laminar boundary layer with suction: (a) on the flat plate with continuous suction according to the rule $v_o \sim 1/\sqrt{x}$, (b) on the flat plate with uniform suction

v_0 = const., (c) on the flat plate with an impinging jet with uniform suction. It became obvious that the stability of the boundary layer is greatly increased by suction, on the other hand greatly reduced by blowing. While the suction quantities are increased slightly, the critical Reynolds number increases greatly and approaches the value found by Bussmann-Münz $(U_0\delta^*/\nu)_{crit}$ = 70,000 for the asymptotic suction profile. Then the minimum suction quantities necessary for maintaining the laminar boundary layer were determined; they were $c_Q = 1.1 \times 10^{-4}$ to 2.8×10^{-4} for the plate with continuous suction and 1.18×10^{-4} for the plate with uniform suction. The drag reduction obtained by maintaining the laminar boundary layer at $Re = 10^7$ is 80 percent of the turbulent drag without suction.

Translated by Mary L. Mahler
National Advisory Committee
for Aeronautics

VIII. BIBLIOGRAPHY

1. A. Betz: Beeinflussung der Reibungsschicht und ihre praktische Verwertung. Schriften der Deutschen Akademie der Luftfahrtforschung, Heft 49 (1942); vgl. auch Jahrbuch der Deutschen Akedemit der Luftfahrtforschung 1939/40, S. 246.

2. K. Bussmann u. H. Münz: Die Stabilität der laminaren Reibungsschicht mit Absaugung. Jahrbuch 1942 der Deutschen Luftfahrtforschung, S. I 36.

3. H. Schlichting u. K. Bussmann: Exakte Lösungen für die laminare Grenzschicht mit Absaugung und Ausblasen. Schriften der Deutschen Akademie der Luftfahrtforschung, Bd. 7B, 1943, Heft 2.

4. R. Iglisch: Exakte Lösungen für die laminare Grenzschicht an der längsangeströmten ebenen Platte mit homogener Absaugung. Bericht 43/22 des Aerodyn. Instituts der T. H. Braunschweig. UM 2061.

5. H. Schlichting: Die Grenzschicht mit Absaugung und Ausblasen. Luftfahrtforschung 1942, S. 179.

6. H. Schlichting: Ueber die theoretische Berechnung der kritischen Reynoldsschen Zahl einer Reibungsschicht in beschleunigter und verzögerter Strömung. Jahrbuch 1940 der deutschen Luftfahrtforschung, S. I 197.

7. H. Holstein: Messungen zur Laminarhaltung der Grenzschicht durch Absaugung an einem Tragflügel mit Profil NACA 0012/64. Bericht der Aerodynamischen Versuchsanstalt Göttingen. FB 1654, (1942).

8. H. Schlichting: Die Beeinflussung der Grenzschicht durch Absaugung und Ausblasen. Jahrbuch 1943/44 der Deutschen Akademie der Luftfahrtforschung.

9. J. Ackeret, M. Ras, W. Pfenninger: Verhinderung des Turbulentwerdens einer Grenzschicht durch Absaugung. Naturwissenschaften Bd. 29 (1941), S. 622.

10. W. Tollmien: Ueber die Entstehung der Turbulenz. Nachr. Ges. Wiss. Göttingen, Math. Phys. Klasse 1929.

TABLE 1

APPROXIMATION OF THE VELOCITY PROFILES FOR VARIOUS C, $\sqrt{\xi}$ AND C_o OF THE THREE INVESTIGATED FLOWS ACCORDING TO EQUATION (9): $\frac{u}{U} = 1 - p\left(a - \frac{y}{\delta}\right)^n$

		C	p	a	n
Flat plate with continuous suction $v_o \sim 1/\sqrt{x}$		-0.25	1.238	0.95	2
		0	1.000	1.015	2
		.5	1.000	1.00	2
		1	.133	1.656	4
		1.5	.137	1.642	4
	ξ	$\sqrt{\xi}$	p	a	n
Flat plate with uniform suction v_o = const.	0	0	1.000	1.015	2
	.005	.0707	1.068	.968	2
	.02	.141	1.042	.980	2
	.08	.283	1.072	.966	2
	.18	.424	.1296	1.667	4
	.32	.566	.1316	1.660	4
	.5	.707	.1335	1.654	4
	∞	∞	.00254	4.46	4
		C_o	p	a	n
Plane stagnation flow with uniform suction		-3.1905	1.0330	0.9839	2
		-1.198	.100	.954	2
		0	.1375	1.642	4
		.5	.1375	1.642	4
		1.095	.1406	1.633	4
		1.9265	.1446	1.622	4

TABLE 2

NUMERICAL VALUES OF THE NEUTRAL STABILITY CURVES OF THE PLATE FLOW WITH CONTINUOUS SUCTION $v_o \sim 1/\sqrt{x}$

C	c/U_o	y_K/δ^*	$\alpha\delta^*$	$\frac{U_o\delta^*}{\nu} \times 10^{-3}$
$\frac{1}{4}$	0.20	0.387	0.092	3.350
	.25	.483	.120	1.373
	.368	.696	.204	.341
WP			.308	∞
	.40	.756	.337	1.498
Asymptote	.40	.756	.234	.249
	.45	.846	.364	.495
	.45	.846	.267	.217
	.47	.879	.365	.367
$\frac{1}{2}$	0.05	0.084	.038	8837
	.05	.084	.0185	1920
	.10	.150	.073	550
	.10	.150	.032	206
	.15	.228	.101	105
	.15	.228	.051	43.8
	.20	.312	.132	26.2
	.20	.312	.075	13.7
	.25	.390	.155	13.5
	.25	.390	.101	6.14
	.30	.474	.174	5.30
	.30	.474	.142	5.33
	.31	.498	.170	3.06
1	0.05	0.069	0.038	13900
	.05	.069	.021	2764
	.10	.138	.071	709
	.10	.138	.035	246
	.15	.207	.094	115
	.15	.207	.058	53.2
	.20	.280	.127	29.0
	.20	.280	.080	18.92
	.25	.357	.131	9.98
$\frac{3}{2}$	0.05	0.022	0.037	11300
	.05	.022	.017	3770
	.10	.044	.077	571
	.10	.044	.035	305
	.15	.067	.100	102
	.15	.067	.055	63.2
	.20	.090	.114	32.1
	.20	.090	.086	22.5

TABLE 3

NUMERICAL VALUES OF THE NEUTRAL STABILITY CURVES OF THE ONCOMING PLATE FLOW WITH UNIFORM SUCTION

ξ	$\frac{c}{U_o}$	$\alpha\delta^*$	$\frac{U_o\delta^*}{\nu} \times 10^{-3}$
0	0.10	0.036	118
	.20	.077	7.20
	.20	.149	37.7
	.25	.101	3.01
	.25	.188	12.0
	.30	.129	1.53
	.30	.223	4.61
	.325	.143	1.15
	.325	.238	3.29
	.35	.159	.893
	.35	.252	2.07
	.375	.181	.736
	.375	.264	1.42
	.40	.205	.633
	.40	.274	1.02
	.42	.239	.605
	.42	.273	.713

TABLE 3 - Continued

NUMERICAL VALUES OF THE NEUTRAL STABILITY CURVES OF

THE ONCOMING PLATE FLOW WITH UNIFORM SUCTION - Continued

ξ	$\frac{c}{U_o}$	$\frac{y_K}{\delta^*}$	$\alpha\delta^*$	$\frac{U_o\delta^*}{\nu} \times 10^{-3}$
0.005	0.10	0.055	0.076	630
	.10	.055	.0365	131
	.20	.114	.157	22.7
	.20	.114	.083	7.9
	.30	.173	.224	3.3
	.30	.173	.145	1.86
	.35	.203	.237	1.51
	.35		.196	1.16
.02	.10	.053	.074	778
	.10	.053	.033	198.5
	.20	.108	.145	28.9
	.20	.108	.074	12.8
	.25	.138	.176	9.3
	.25	.138	.108	5.06
	.30	.167	.200	3.85
	.30	.167	.143	2.59
.08	.10	.050	.073	543
	.10	.050	.034	204
	.20	.100	.134	26.6
	.20	.100	.080	15.3
	.25	.127	.160	9.67
	.25	.127	.111	6.65
	.275	.1405	.168	6.17
	.275	.1405	.132	4.67
	.295	.151	.163	3.95

TABLE 3 - Concluded

NUMERICAL VALUES OF THE NEUTRAL STABILITY CURVES OF

THE ONCOMING PLATE FLOW WITH UNIFORM SUCTION - Concluded

ξ	$\frac{c}{U_o}$	$\frac{y_K}{\delta^*}$	$\alpha\delta^*$	$\frac{U_o\delta^*}{\nu} \times 10^{-3}$
0.18	0.10	0.047	0.073	603.3
	.10	.047	.046	89.7
	.20	.096	.125	26.9
	.20	.096	.082	16.3
	.25	.120	.138	10.13
	.25	.120	.105	8.67
.32	0.05	0.0225	0.037	12230
	.05	.0225	.014	4277
	.15	.068	.099	96.7
	.15	.068	.056	60.2
	.20	.092	.122	28.9
	.20	.092	.089	22.6
.5	0.05	0.022	0.038	10640
	.05	.022	.017	3727
	.15	.066	.094	107.0
	.15	.066	.056	67.5
	.20	.088	.111	31.5
	.20	.088	.034	24.9
∞	0.025	0.0253	0.0176	43200
	.025	.0253	.0080	106400
	.09	.0943	.0618	1500
	.09	.0943	.0326	755
	.15	.163	.0935	147
	.15	.163	.0605	113
	.175	.192	.088	70

TABLE 4

NUMERICAL VALUES OF THE NEUTRAL STABILITY CURVES OF THE PLANE STAGNATION FLOW WITH UNIFORM SUCTION

C_o	$\frac{c}{U_o}$	$\alpha\delta^*$	$\frac{U_o\delta^*}{\nu} \times 10^{-3}$
-3.1905	0.15	0.109	77.6
	.15	.054	25.1
	.20	.144	26.7
	.20	.079	8.6
	.30	.207	3.70
	.30	.134	2.02
	.35	.237	1.58
	.35	.200	1.12
-1.198	.10	.071	653
	.10	.034	218
	.15	.106	107
	.15	.053	46.3
	.20	.142	27.4
	.20	.079	14.3
	.25	.171	9.63
	.25	.114	6.33
	.29	.165	4.46
0	.05	.033	1470
	.05	.016	440
	.10	.069	711
	.10	.034	292
	.15	.098	114
	.15	.055	64.8
	.20	.119	31
	.20	.082	18.1
	.23	.125	14.8
	.23	.102	13.8

TABLE 4 - Concluded

NUMERICAL VALUES OF THE NEUTRAL STABILITY CURVES OF THE PLANE STAGNATION FLOW WITH UNIFORM SUCTION - Concluded

C_o	$\frac{c}{U_o}$	$\alpha\delta^*$	$\frac{U_o\delta^*}{\nu} \times 10^{-3}$
0.5	0.05	0.032	15500
	.05	.007	11740
	.10	.065	890
	.10	.031	357
	.15	.094	138.6
	.15	.053	79.5
	.20	.120	33.4
	.20	.078	26.5
	.22	.114	22.7
	.22	.101	19.1
1.095	.05	.029	23493
	.05	.013	7512
	.10	.067	951
	.10	.032	418
	.15	.093	137.6
	.15	.055	83.7
	.20	.112	35.6
	.20	.083	29.2
	.215	.106	24.0
1.9265	.05	.031	21190
	.05	.014	8156
	.10	.063	714
	.10	.032	418.5
	.15	.091	124.8
	.15	.055	83.5
	.175	.104	59.5
	.175	.073	49.7
	.19	.093	38.0

TABLE 5

THE CRITICAL REYNOLDS NUMBERS AS FUNCTIONS OF C, $\sqrt{\xi}$,

AND C_o FOR THE THREE INVESTIGATED FLOWS

	$C = c_Q\sqrt{\frac{U_o l}{\nu}}$	$\frac{\delta^*}{\vartheta}$	$\left(\frac{U_o\delta^*}{\nu}\right)_{crit}$	$\left(\frac{U_o x}{\nu}\right)_{crit}$
Flat plate with continuous suction $v_o \sim 1/\sqrt{x}$	-0.25	2.77	204	1.03×10^4
	0	2.59	575	1.10×10^5
	.5	2.41	2986	5.25×10^6
	1	2.29	9550	8.31×10^7
	1.5	2.22	19100	4.90×10^8
	Asymptotic suction profile	2	70000	---
	$\sqrt{\xi} = \frac{-v_o}{U_o}\sqrt{\frac{U_o x}{\nu}}$	$\frac{\delta^*}{\vartheta}$	$\left(\frac{U_o\delta^*}{\nu}\right)_{crit}$	
Flat plate with uniform suction v_o = const.	0	2.59	575	
	.0707	2.53	1122	
	.141	2.47	1820	
	.283	2.39	3935	
	.424	2.31	7590	
	.566	2.25	13500	
	.707	2.21	21900	
		2	70000	
	$C_o = \frac{-v_o}{\sqrt{u_1\nu}}$	$\frac{\delta^*}{\vartheta}$	$\left(\frac{U_o\delta^*}{\nu}\right)_{crit}$	
Plane stagnation flow with uniform suction	-3.1905	2.538	707	
	-1.198	2.352	4460	
	0	2.218	12300	
	.5	2.172	17360	
	1.095	2.126	27700	
	1.9265	2.088	38000	

TABLE 6

DRAG REDUCTION AT VARIOUS REYNOLDS NUMBERS FOR THE PLATE FLOW WITH CONTINUOUS ($v_o \sim 1/\sqrt{x}$) AND WITH UNIFORM SUCTION

	$\frac{U_o l}{\nu}$	C_{crit}	$c_{Q crit} \times 10^3$	Full turb. $c_f \times 10^3$	Laminar with suction $c_f \times 10^3$	$\Delta c_f \times 10^3$	$\frac{\Delta c_f}{c_f \text{ full turbulent}}$
Flat plate with continuous suction $v_o \sim 1/\sqrt{x}$	2×10^6	0.4	0.28	4.0	1.4	2.6	0.65
	5×10^6	.5	.225	3.3	.95	2.35	.71
	10^7	.65	.205	2.9	.8	2.1	.75
	2×10^7	.8	.18	2.7	.6	2.1	.78
	5×10^7	.9	.13	2.4	.4	2.0	.83
	10^8	1.05	.11	2.2	.3	1.9	.86
Flat plate with uniform suction v_o = const.	10^6	---	0.118	4.4	1.5	2.9	0.66
	2×10^6	---		3.8	1.1	2.7	.71
	5×10^6	---		3.3	.8	2.5	.76
	10^7	---		3.0	.6	2.4	.80
	2×10^7	---		2.6	.45	2.15	.83
	5×10^7	---		2.3	.35	1.95	.85
	10^8	---		2.1	.30	1.8	.86

Minimum quantity suction at the plate

$\Delta c_f = (c_f)_{\text{full turb.}} - (c_f)_{\text{laminar with suction}}$

TABLE 7

THE CHARACTERISTIC BOUNDARY-LAYER PARAMETERS OF THE INVESTIGATED LAMINAR VELOCITY PROFILES WITH SUCTION

	$C = c_Q\sqrt{\frac{U_0 l}{\nu}}$	$\delta^*\sqrt{\frac{U_0}{\nu x}}$	$\vartheta\sqrt{\frac{U_0}{\nu x}}$	$\frac{\delta^*}{\vartheta}$	$\frac{\tau_0\delta^*}{\mu U_0}$
Flat plate	-0.25	2.010	0.740	2.77	0.500
with con-		1.721	.664	2.59	.573
tinuous	.5	1.303	.541	2.41	.682
suction	1	1.047	.458	2.29	.763
$v_0 \sim 1/\sqrt{x}$	1.5	.863	.390	2.22	.818
	$\sqrt{\xi} = c_Q\sqrt{\frac{U_0 x}{\nu}}$	$\frac{-v_0\delta^*}{\nu}$	$\frac{-v_0\vartheta}{\nu}$	$\frac{\delta^*}{\vartheta}$	$\frac{\tau_0\delta^*}{\mu U_0}$
Flat plate	0	0	0	2.59	0.571
with	.0707	.114	0.045	2.53	.607
uniform	.141	.211	086	2.47	.631
suction	.212	.303	.125	2.43	.671
v_0 = const.	.283	.381	.160	2.39	.699
	.354	.450	.192	2.35	.726
	.424	.511	.221	2.31	.750
	.495	.566	.248	2.28	.773
	.566	.614	.273	2.25	.794
	.636	.658	.295	2.23	.813
	.707	.695	.315	2.21	.830
	∞	1	.5	2	1
	$C_0 = \frac{-v_0}{\sqrt{u_1\nu}}$	$\delta^*\sqrt{\frac{u_1}{\nu}}$	$\vartheta\sqrt{\frac{u_1}{\nu}}$	$\frac{\delta^*}{\vartheta}$	$\frac{\tau_0\delta^*}{\mu U}$
Plane stag-	-3.1905	1.959	0.772	2.54	0.608
nation flow	-1.198	1.018	.433	2.35	.698
with	0	.648	.292	2.22	.796
uniform	.5	.542	.250	2.17	.836
suction	1.095	.444	.209	2.13	.868
	1.9265	.349	.167	2.09	.917

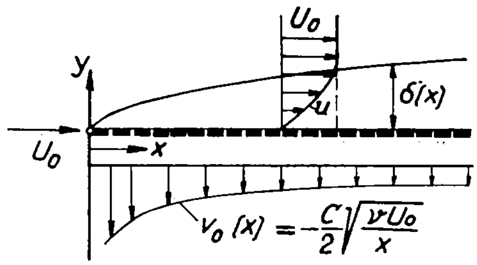

Figure 1. Explanatory chart: Boundary layer at the plate in longitudinal flow with continuous suction according to the rule $v_0(x) = -\frac{c}{2}\sqrt{\frac{\nu U_0}{x}}$.

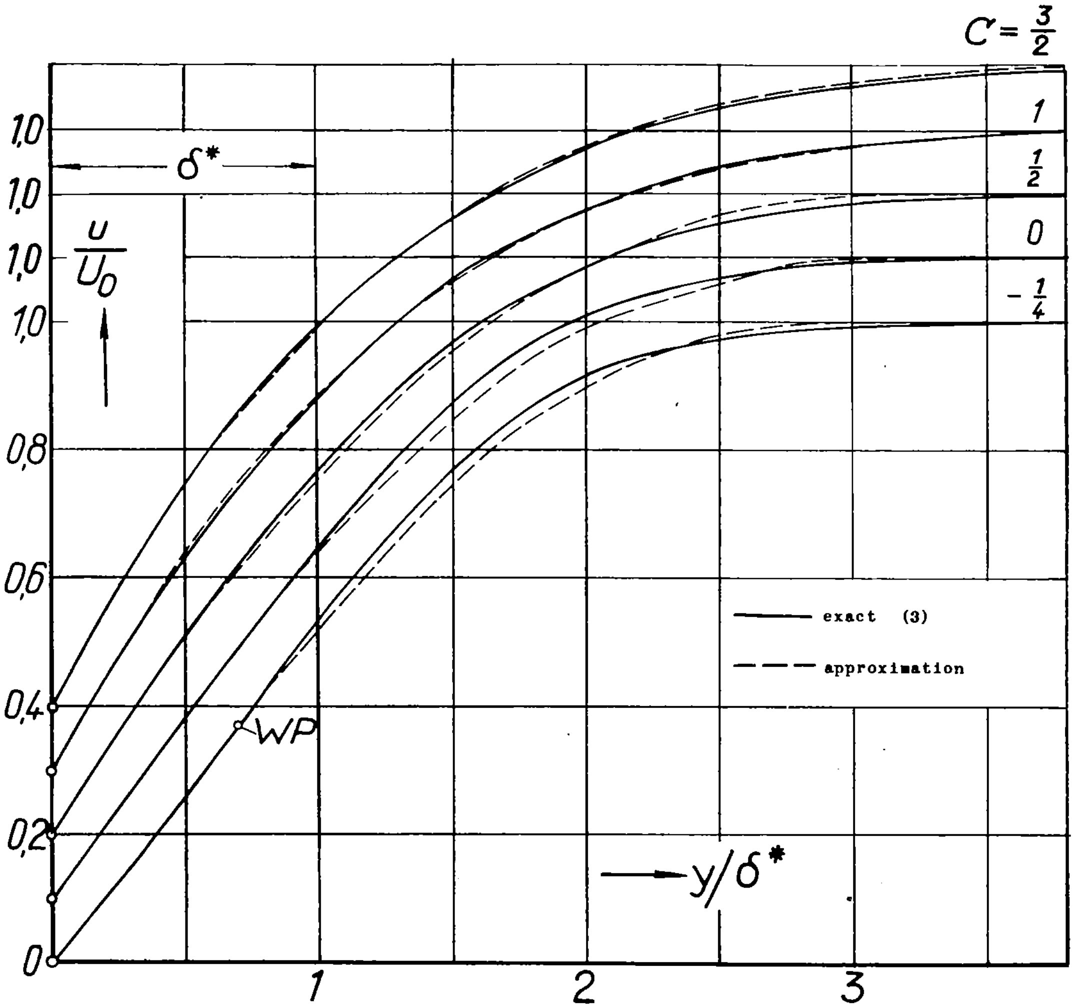

Figure 2. Velocity distributions u/U_0 against y/δ^* for various flow coefficients C of the flow from Fig.1; WP = point of inflection. Comparison with the approximation of equation (9).

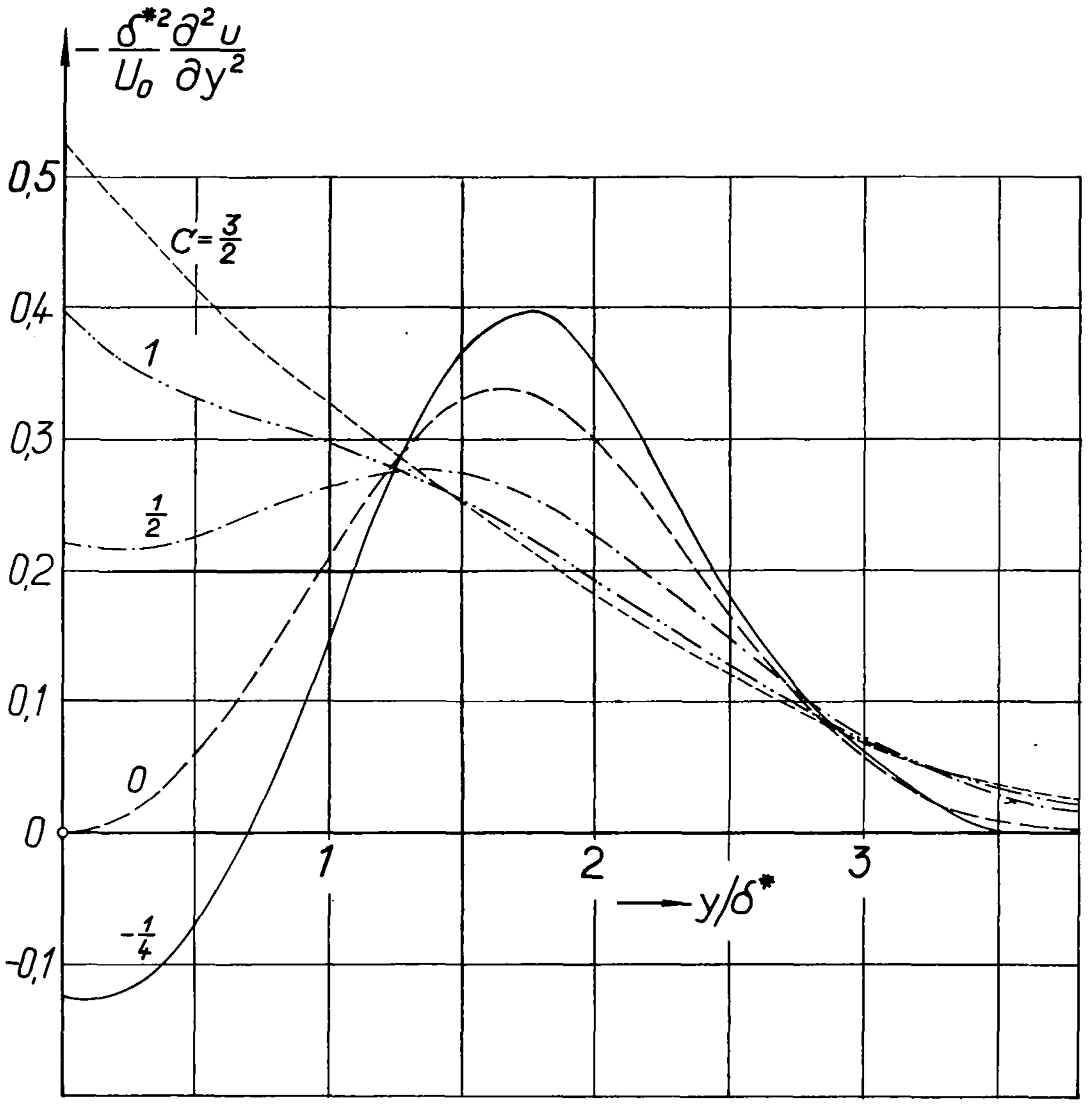

Figure 3. The second derivatives of the velocity distributions from Fig. 2. (C = flow coefficient).

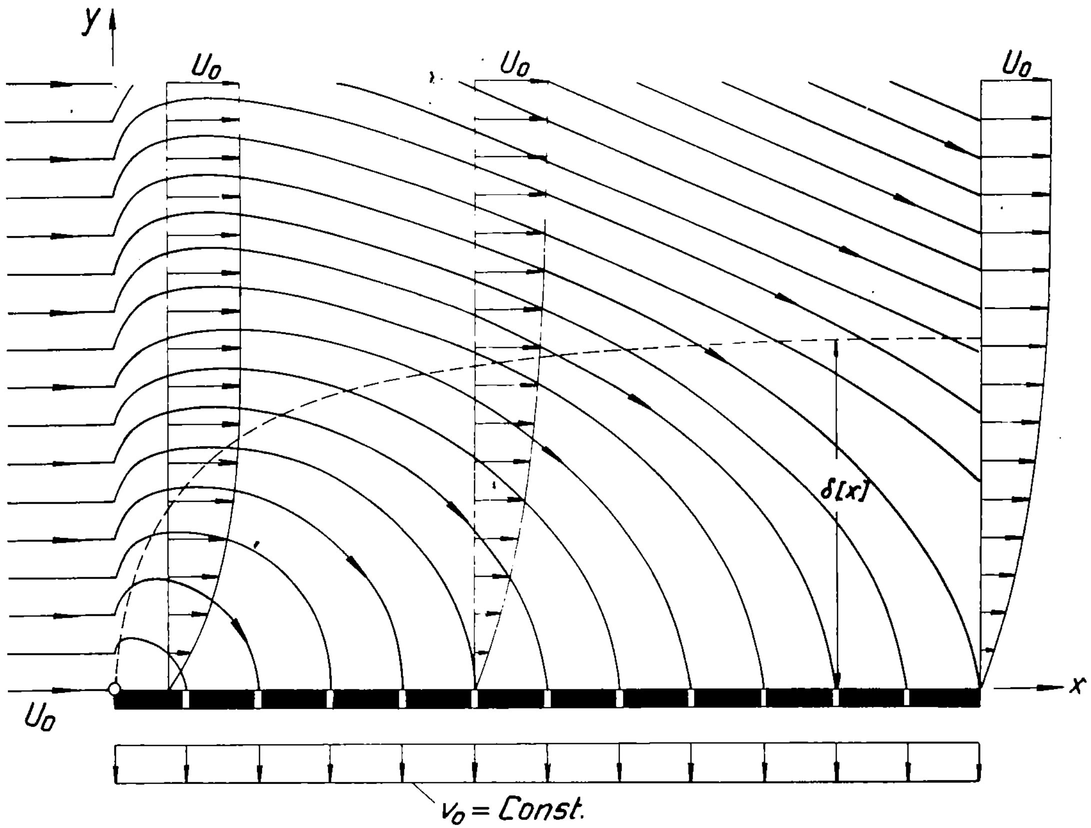

Figure 4. Explanatory chart: Boundary layer of the plate in longitudinal flow with uniform suction $v_0 =$ const.

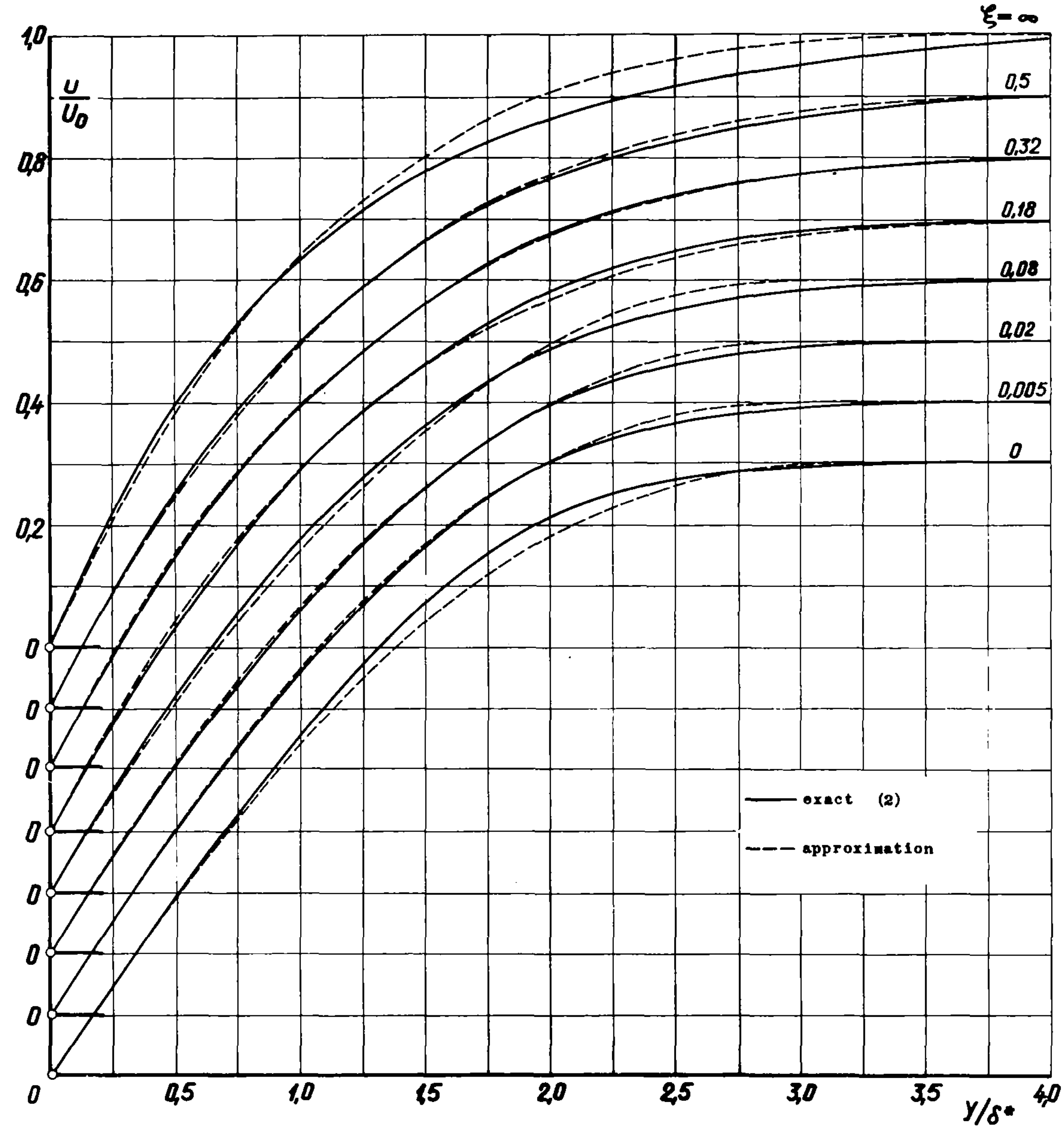

Figure 5. Velocity distributions u/U_0 against y/δ^* for different ξ according to Iglisch [4] ; comparisons with the approximation of equation (9).

$$\xi = \left(\frac{-v_0}{U_0}\right)^2 \quad \frac{U_0 x}{\nu} .$$

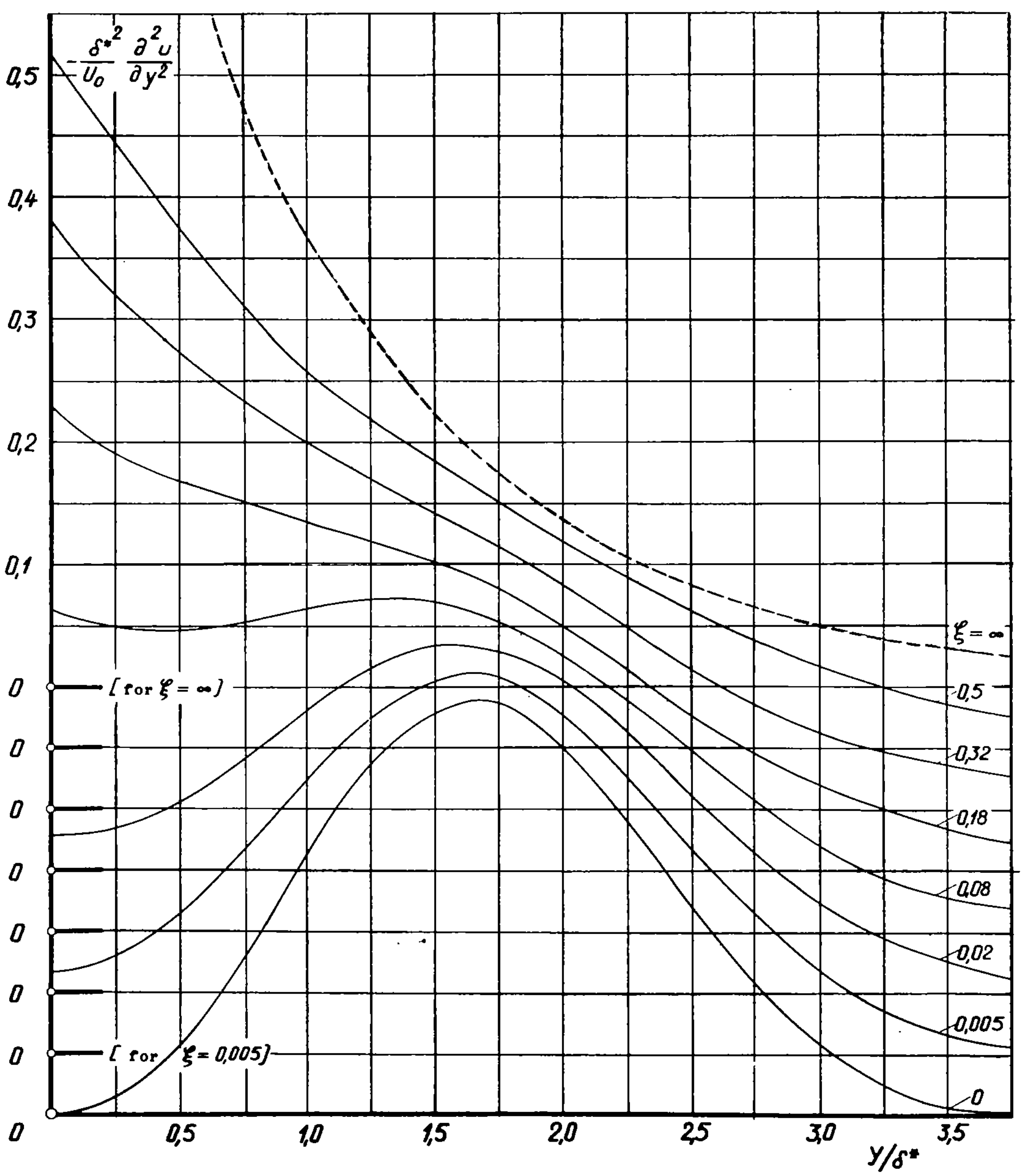

Figure 6. The second derivatives of the velocity distributions of Fig. 5, according to Iglisch [4] .

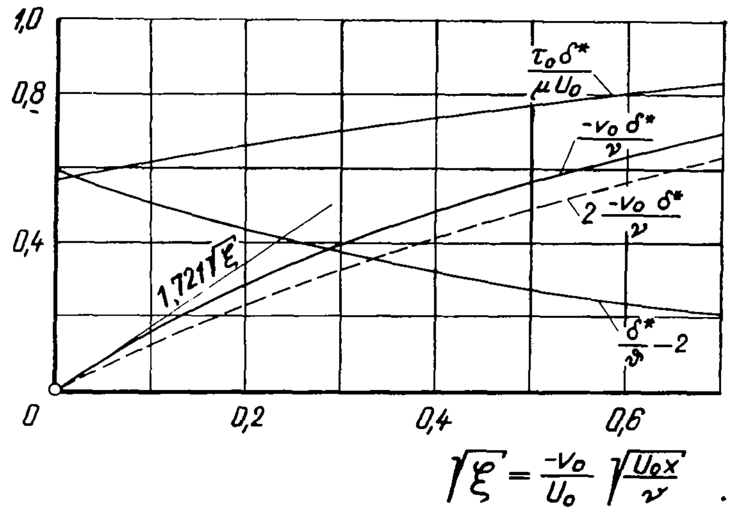

Figure 7. The boundary layer parameters for the plate with uniform suction: $\frac{-v_0\delta^*}{\nu}$, $\frac{-v_0\vartheta}{\nu}$, $\frac{\tau_0\delta^*}{\mu U_0}$ and $\frac{\delta^*}{\vartheta}$ against $\sqrt{\xi}$ according to Iglisch [4]. (Flow Fig.4).

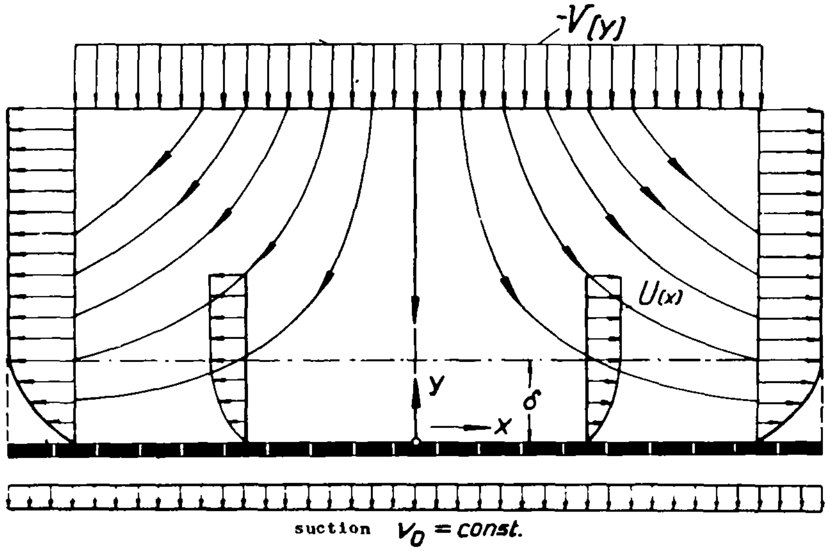

Figure 8. Explanatory chart: Boundary layer of the plane stagnation flow with uniform suction v_0= const.

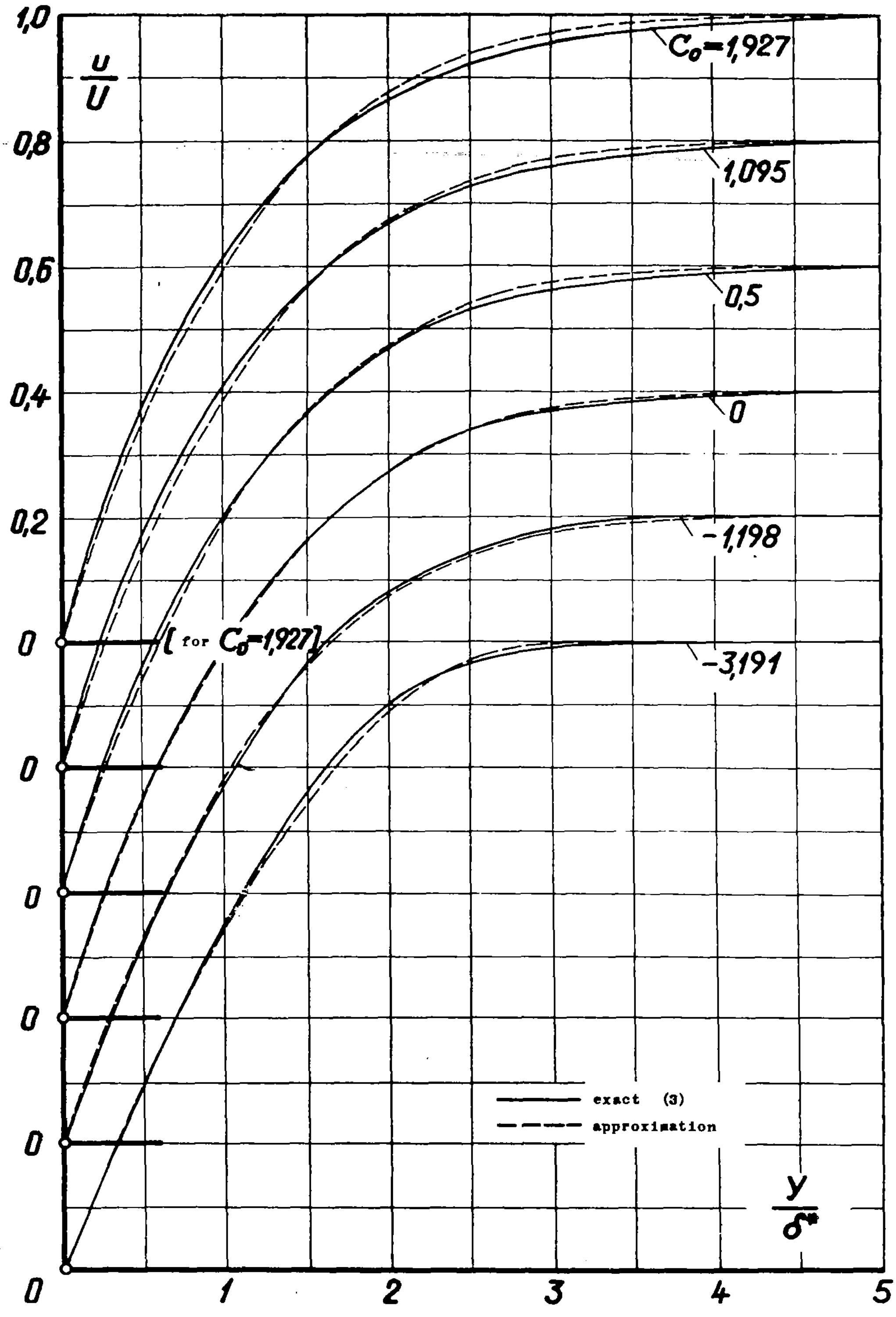

Figure 9. Velocity distribution u/U_o against y/δ^* for different C_o, according to Schlichting-Bussmann [3] ; comparison with the approximation of equation (9).

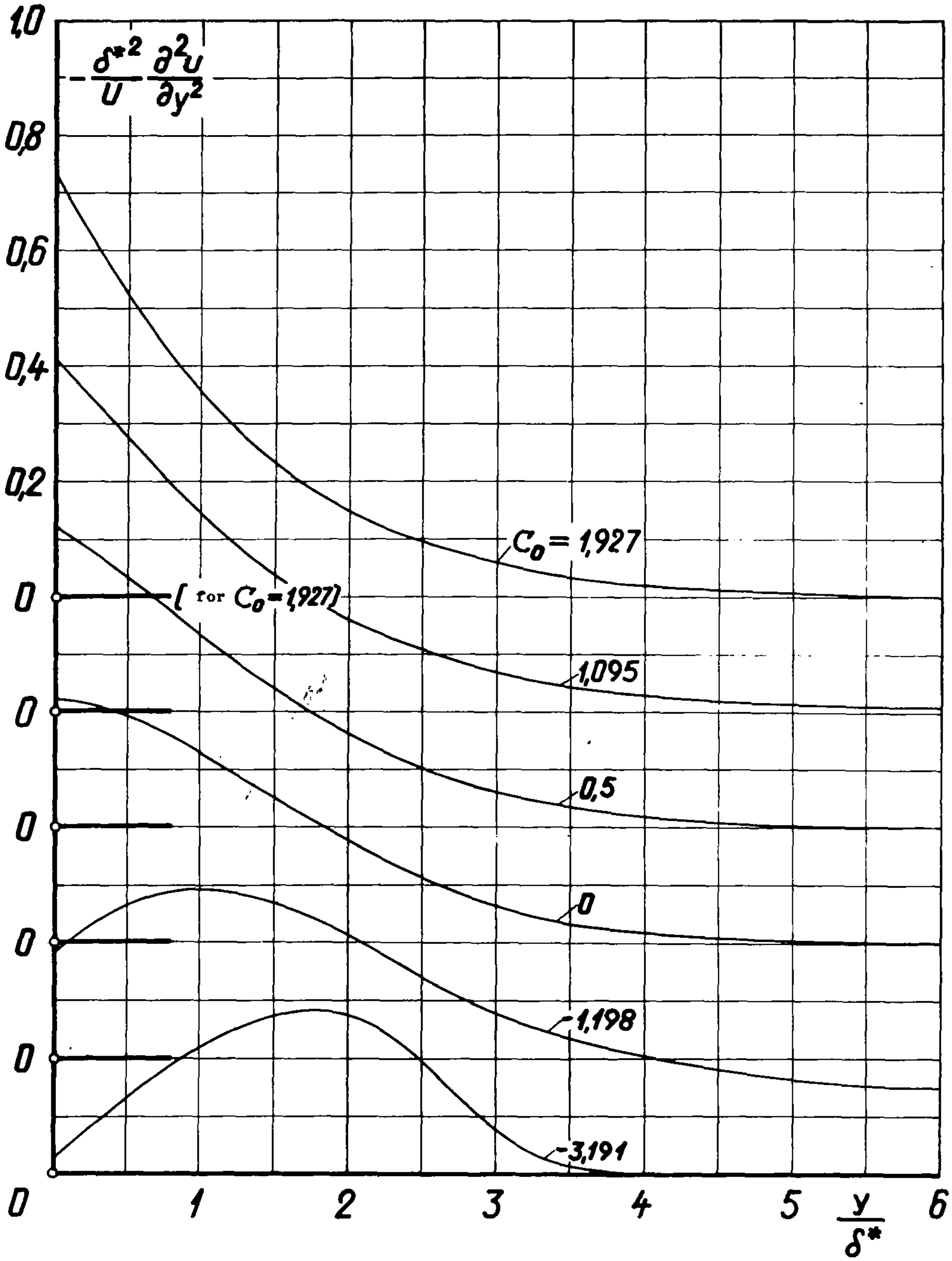

Figure 10. The second derivatives of the velocity distributions from Fig.8 according to Schlichting-Bussmann [3] .

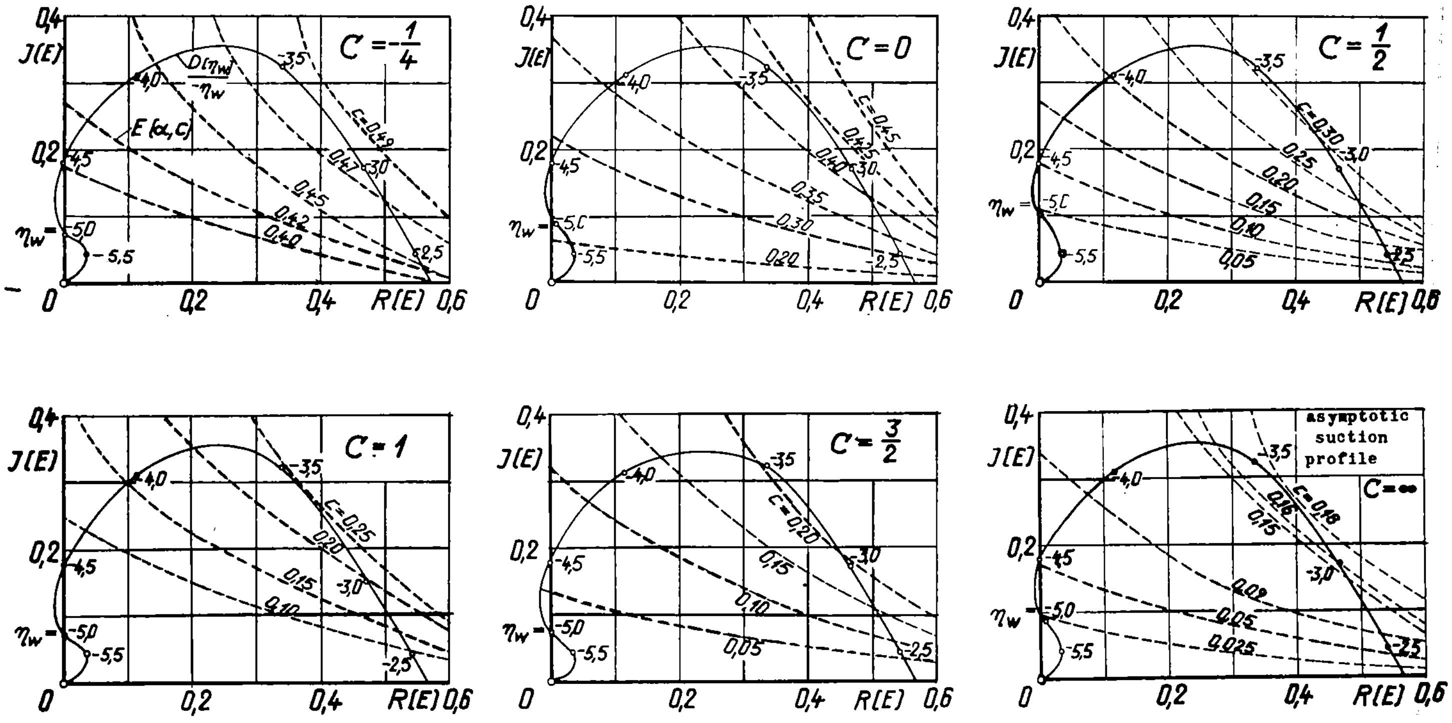

Figure 11. Polar diagrams for the solution of the equation $D(\eta_w)/-\eta_w = E(\alpha, c)$ for the velocity profiles of the flat plate in longitudinal flow with $v_0 \sim 1/\sqrt{x}$; calculation of stability.

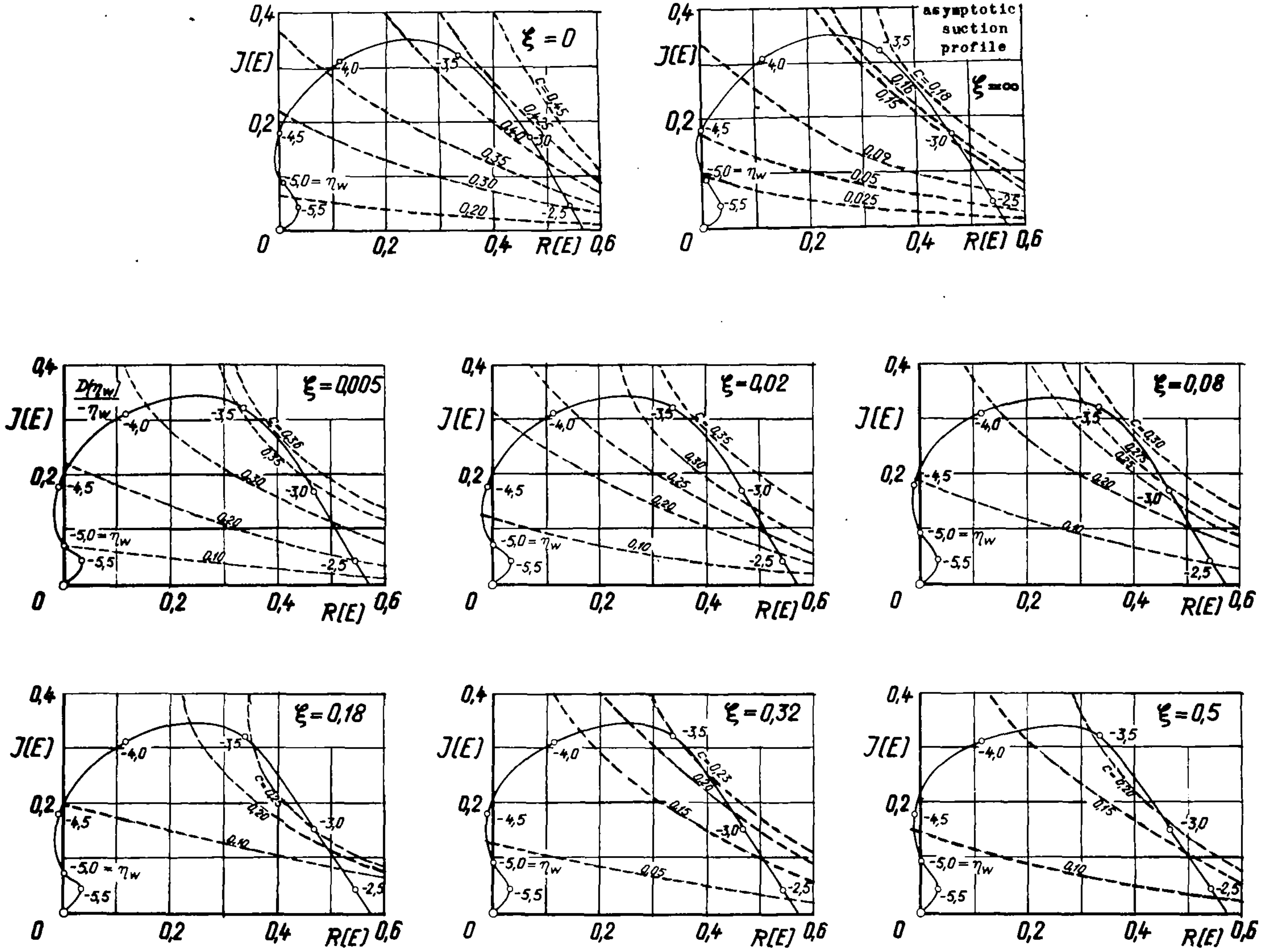

Figure 12. Polar diagrams for the solution of the equation $D(\eta_w)/-\eta_w = E(\alpha, c)$ for the velocity profiles of the flat plate in longitudinal flow with uniform suction; calculation of stability.

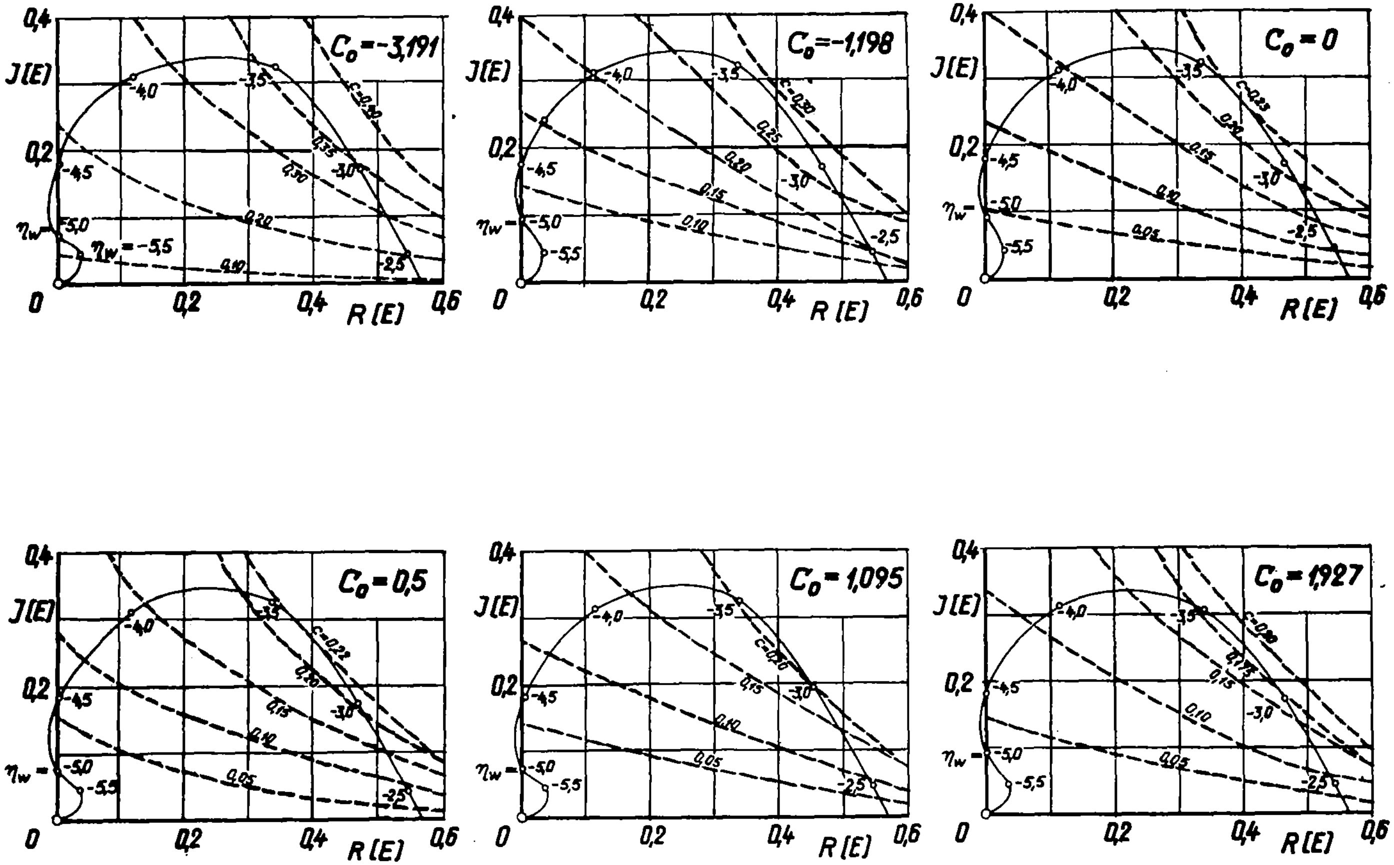

Figure 13. Polar diagrams for the solution of the equation $D(\eta_w)/-\eta_w = E(\alpha, c)$ for the velocity profiles of the plane stagnation flow.

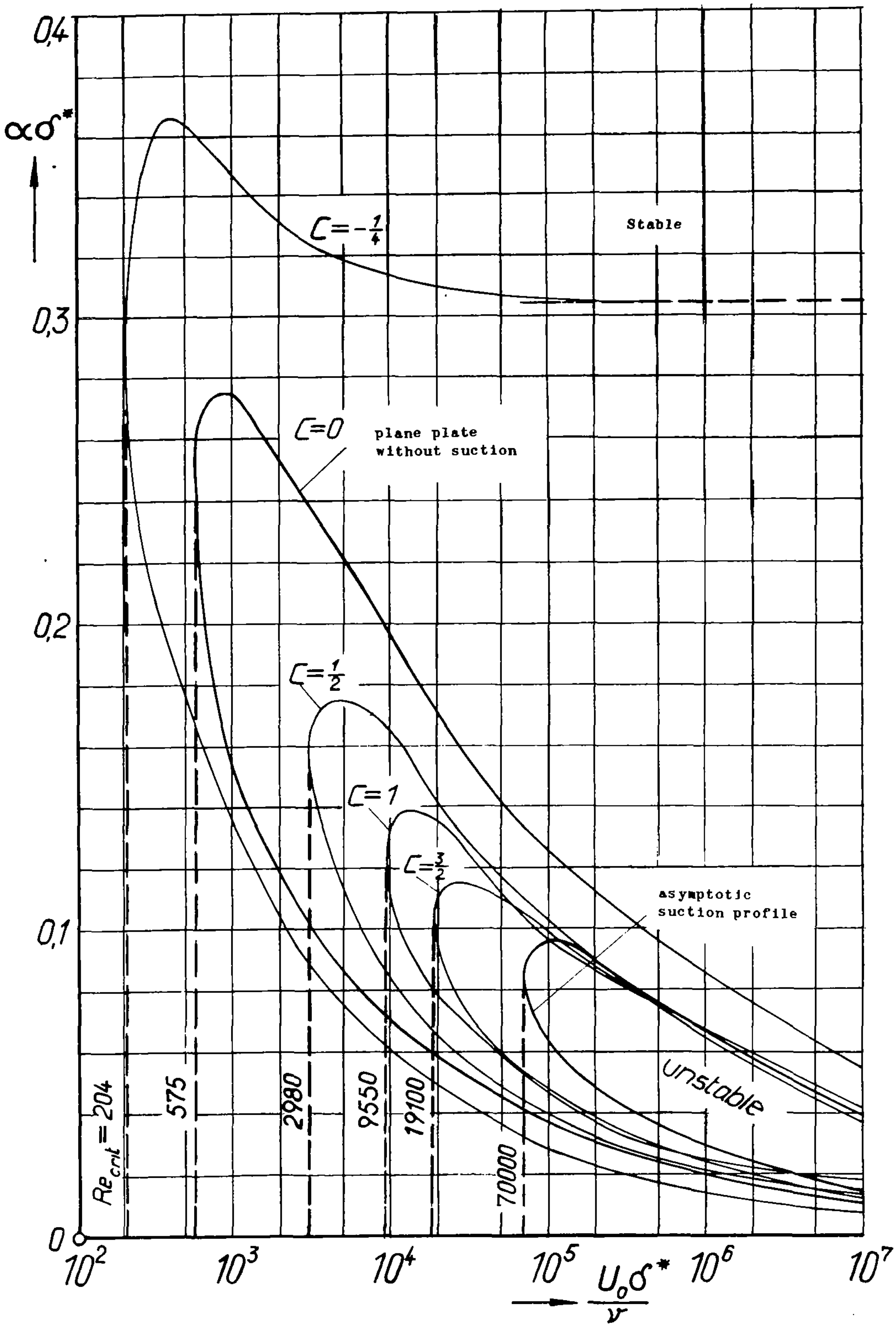

Figure 14. Result of the stability calculation for the flat plate in longitudinal flow with $v_o \sim 1/\sqrt{x}$. The neutral stability curves $\alpha\delta^*$ against $U\delta^*/\nu$ for various flow coefficients C.

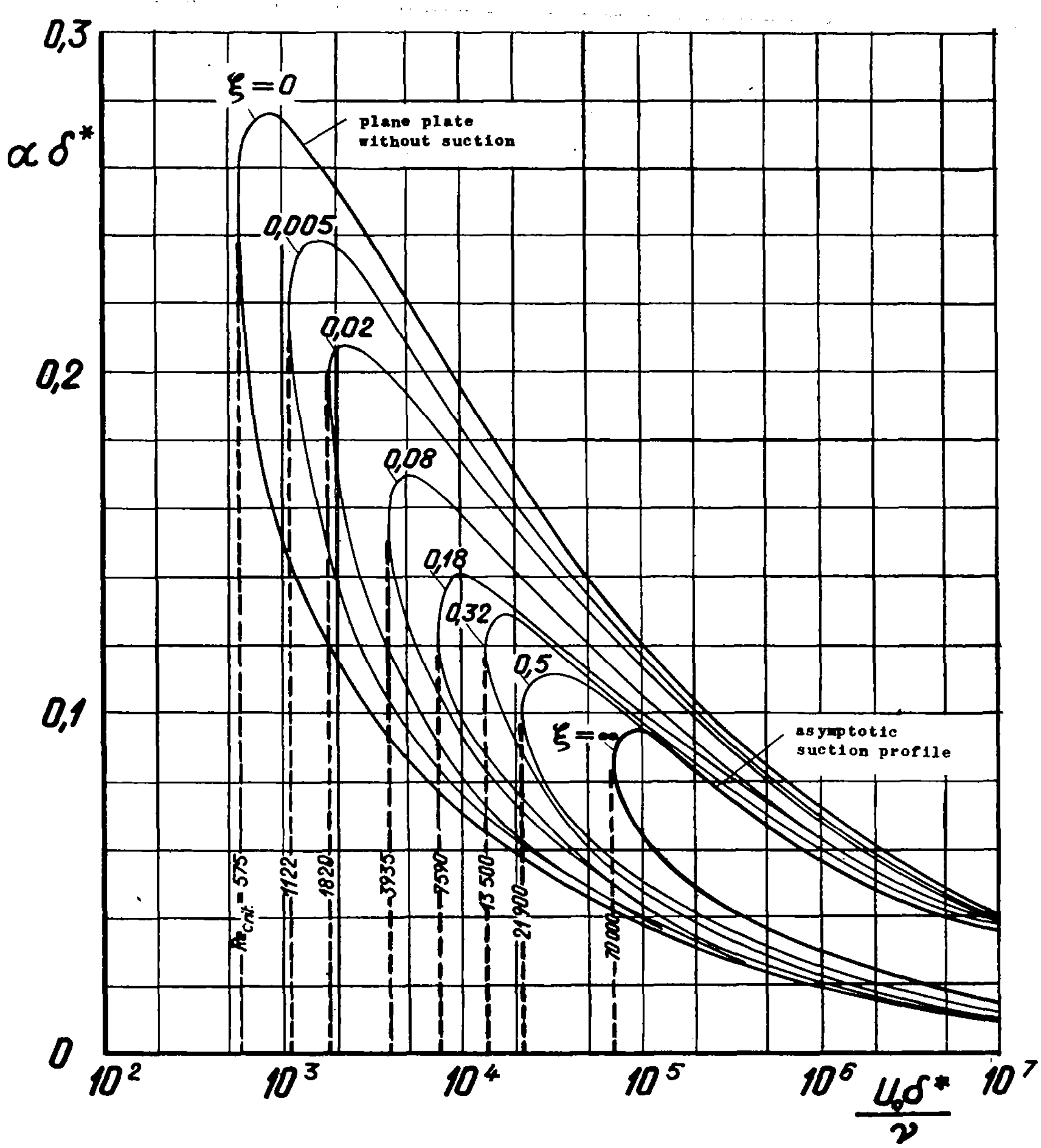

Figure 15. Result of the stability calculation for the plate in longitudinal flow with uniform suction: The neutral stability curves $\alpha\delta^*$ against $U\delta^*/\nu$ for various ξ; $\xi = \left(\frac{-v_o}{U_o}\right)^2 \frac{U_o x}{\nu}$.

$\xi = 0$: Plate without suction (Blasius)

$\xi = \infty$: Asymptotic suction profile.

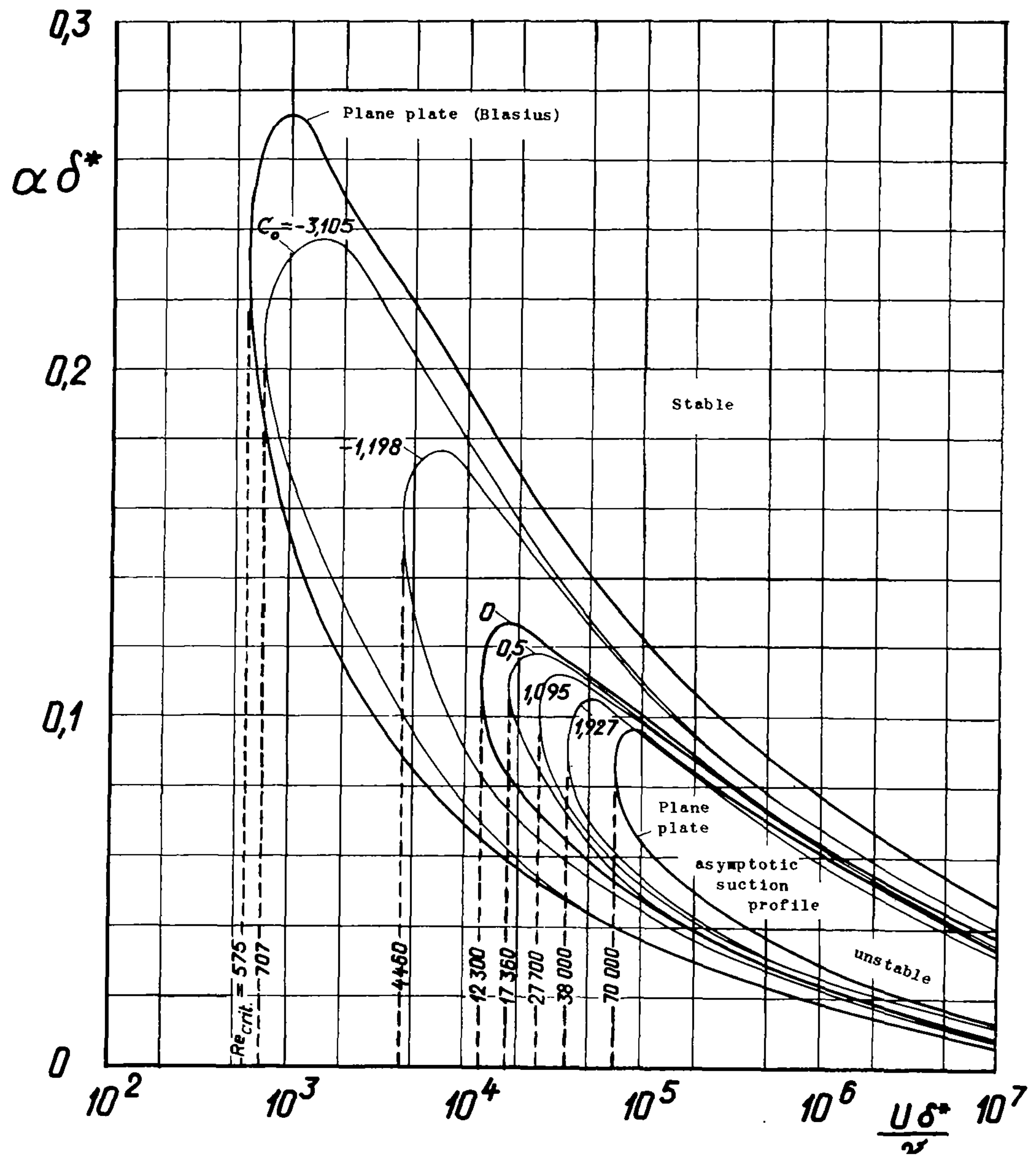

Figure 16. Result of the stability calculation for the plane stagnation flow with uniform suction: The neutral stability curves $\alpha\delta^*$ against $U\delta^*/\nu$ for various flow coefficients $c_o = \frac{-v_o}{\sqrt{u_1\nu}}$.

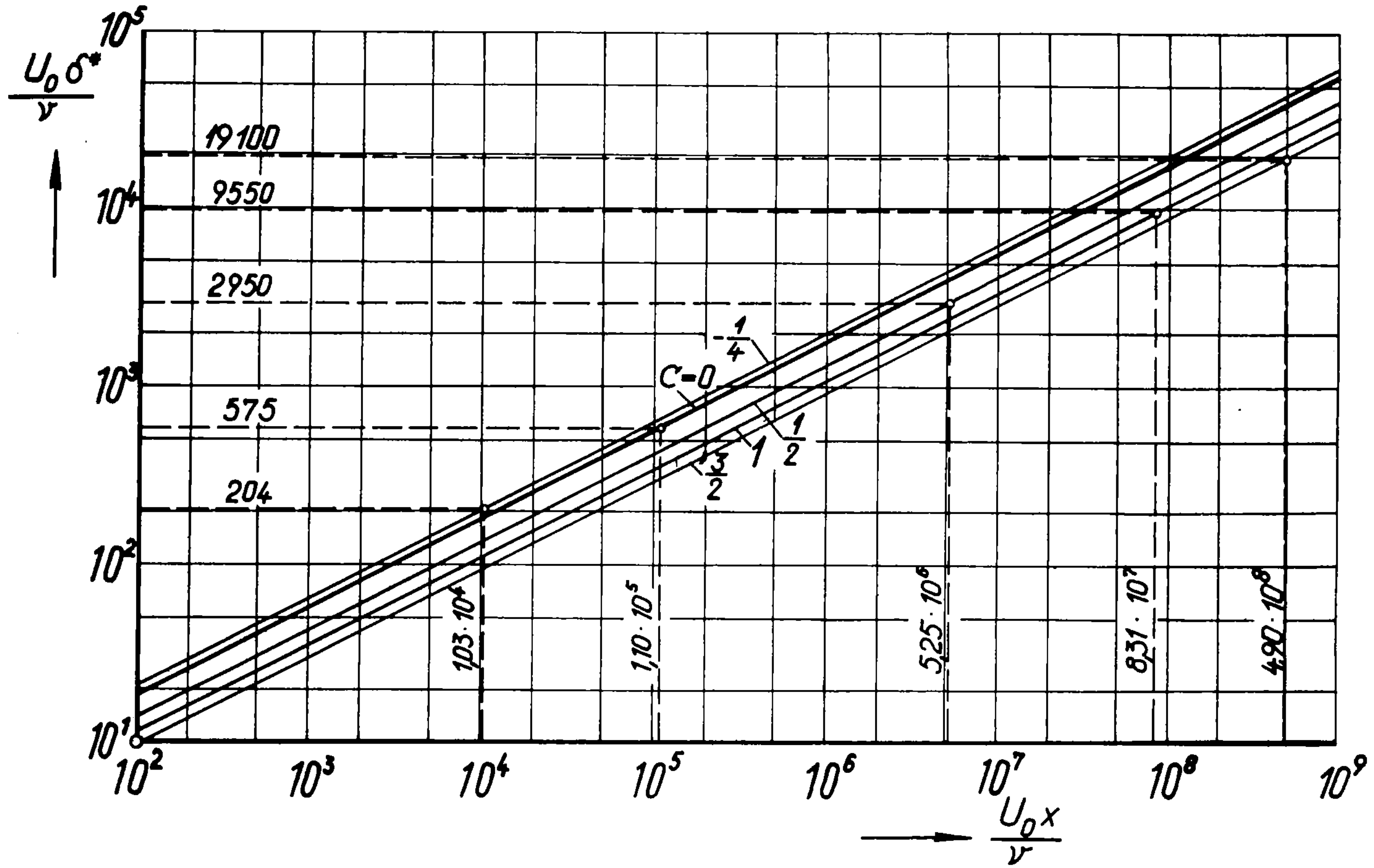

Figure 17. For ascertaining the position of the point of instability $(U_0 x/\nu)_{crit}$ from the calculated critical Reynolds number $(U_0 \delta^*/\nu)_{crit}$ for the plate in longitudinal flow with $v_0 \sim 1/\sqrt{x}$.

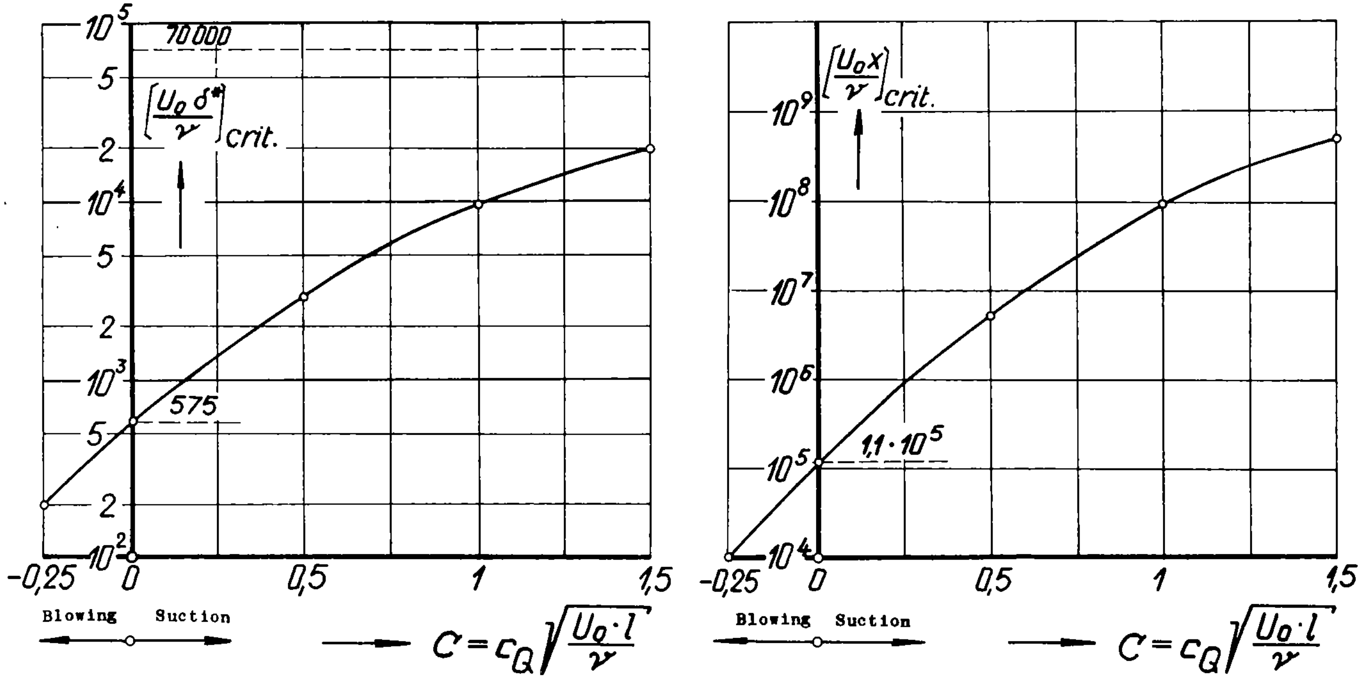

Figure 18. Dependency of the critical Re-numbers $(U_0x/\nu)_{crit}$ and $(U_0\delta^*/\nu)_{crit}$ on the flow coefficient $C = c_Q\sqrt{Re}$ for the plate in longitudinal flow with $v_0 \sim 1/\sqrt{x}$.

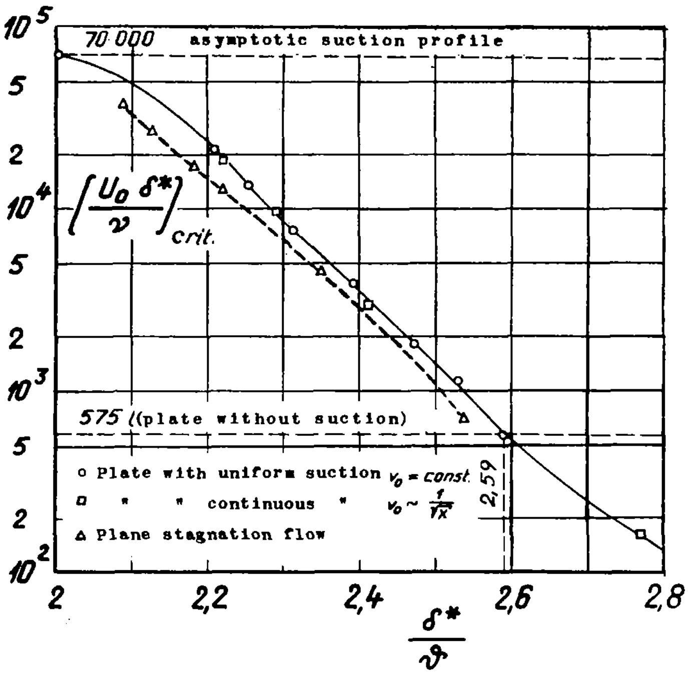

Figure 19. The critical Re-number $(U_0\delta^*/\nu)_{crit}$ as a function of the shape parameter δ^*/ϑ for the plate in longitudinal flow with $v_0 \sim 1/\sqrt{x}$ and $v_0 = \text{const.}$ and the plane stagnation flow.

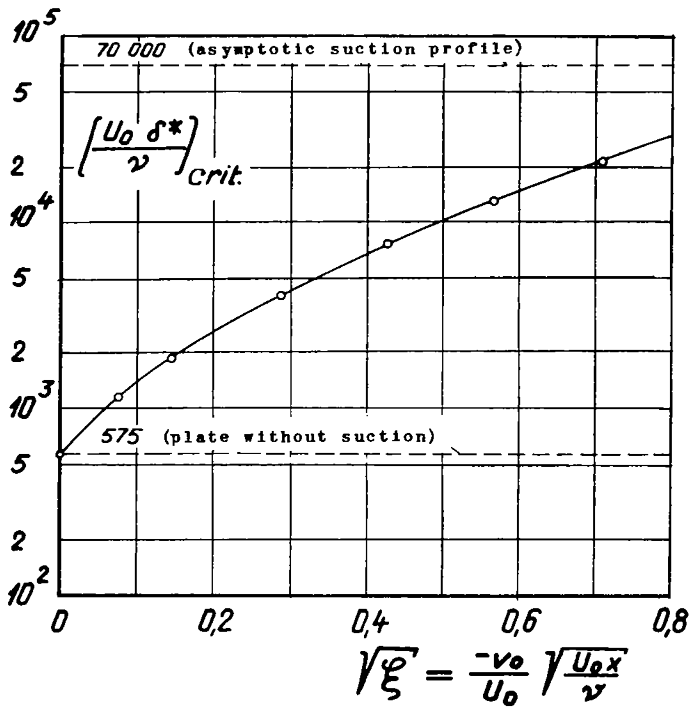

Figure 20. The critical Re-number $(U_0 \delta^* / \nu)_{crit}$ as a function of $\frac{-v_0}{U_0}\sqrt{\frac{U_0 x}{\nu}} = \sqrt{\xi}$ for the flat plate in longitudinal flow with uniform suction.

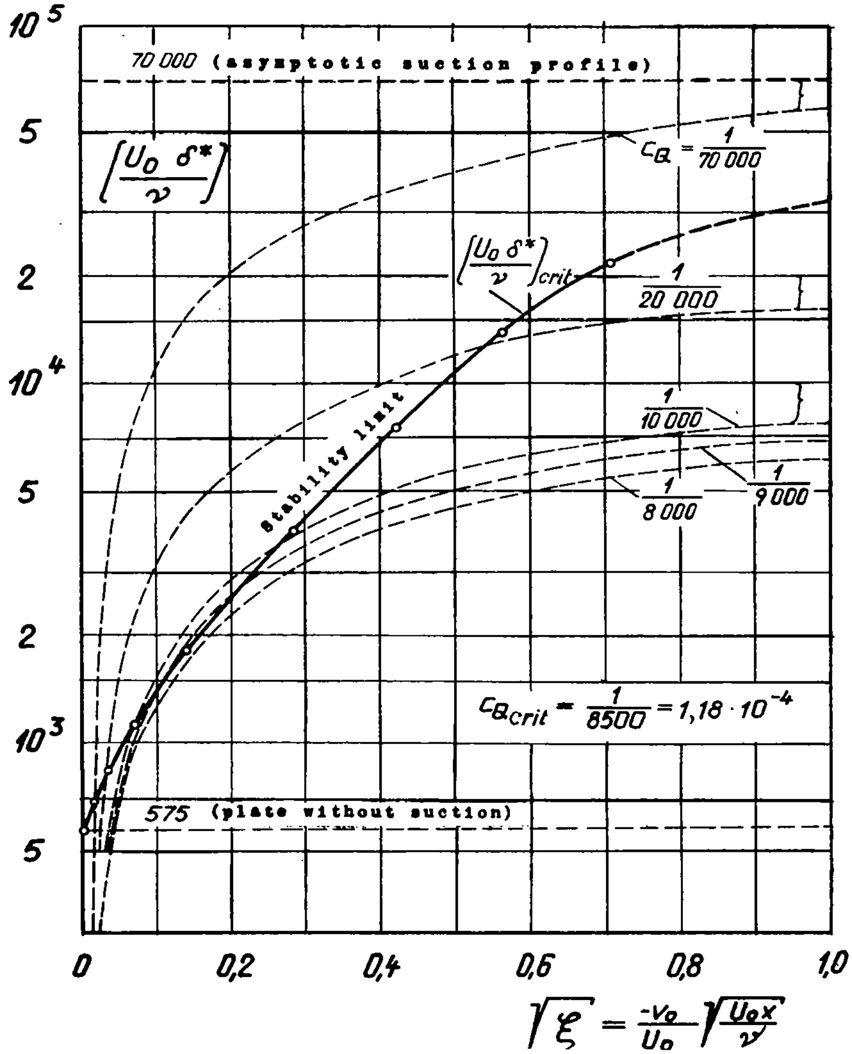

Figure 21. Ascertaining of the critical flow coefficient c_Q for maintaining the laminar flow for the plate in longitudinal flow with uniform suction.

$$\text{Asymptotes:} \quad \left(\frac{U_0\delta^*}{\nu}\right)_\infty = \frac{U_0}{-v_0} = \frac{1}{c_Q} .$$

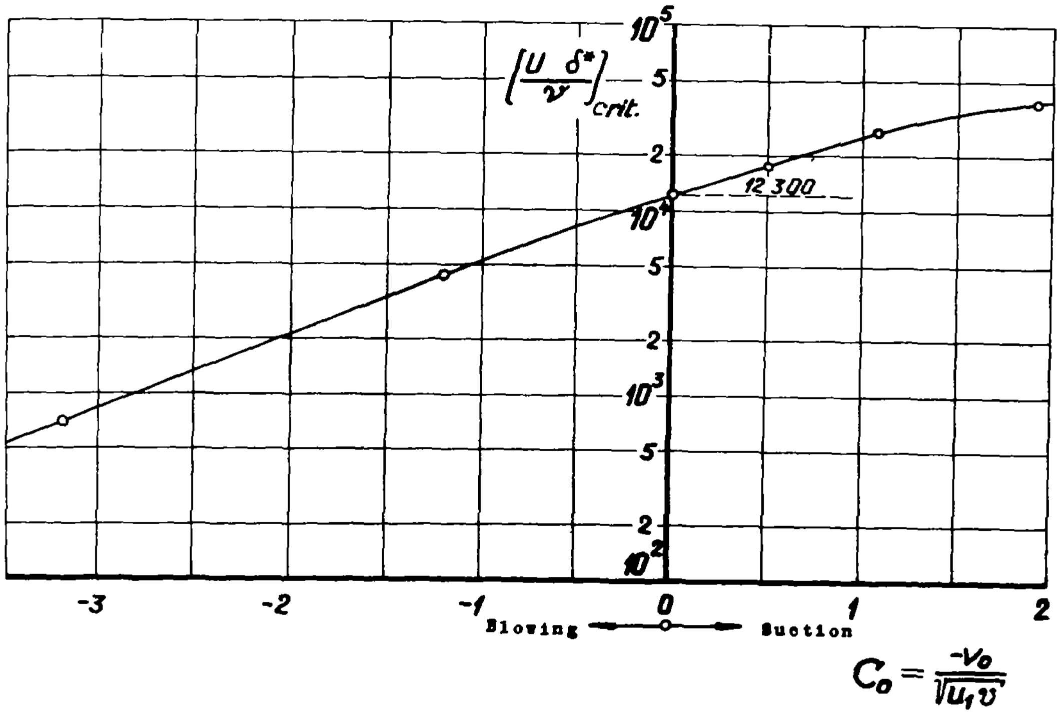

Figure 22. The critical Reynolds number $\left(\frac{U_0 \delta^*}{\nu}\right)_{crit}$ as a function of the flow coefficient C_0 for the plane stagnation flow with uniform suction.

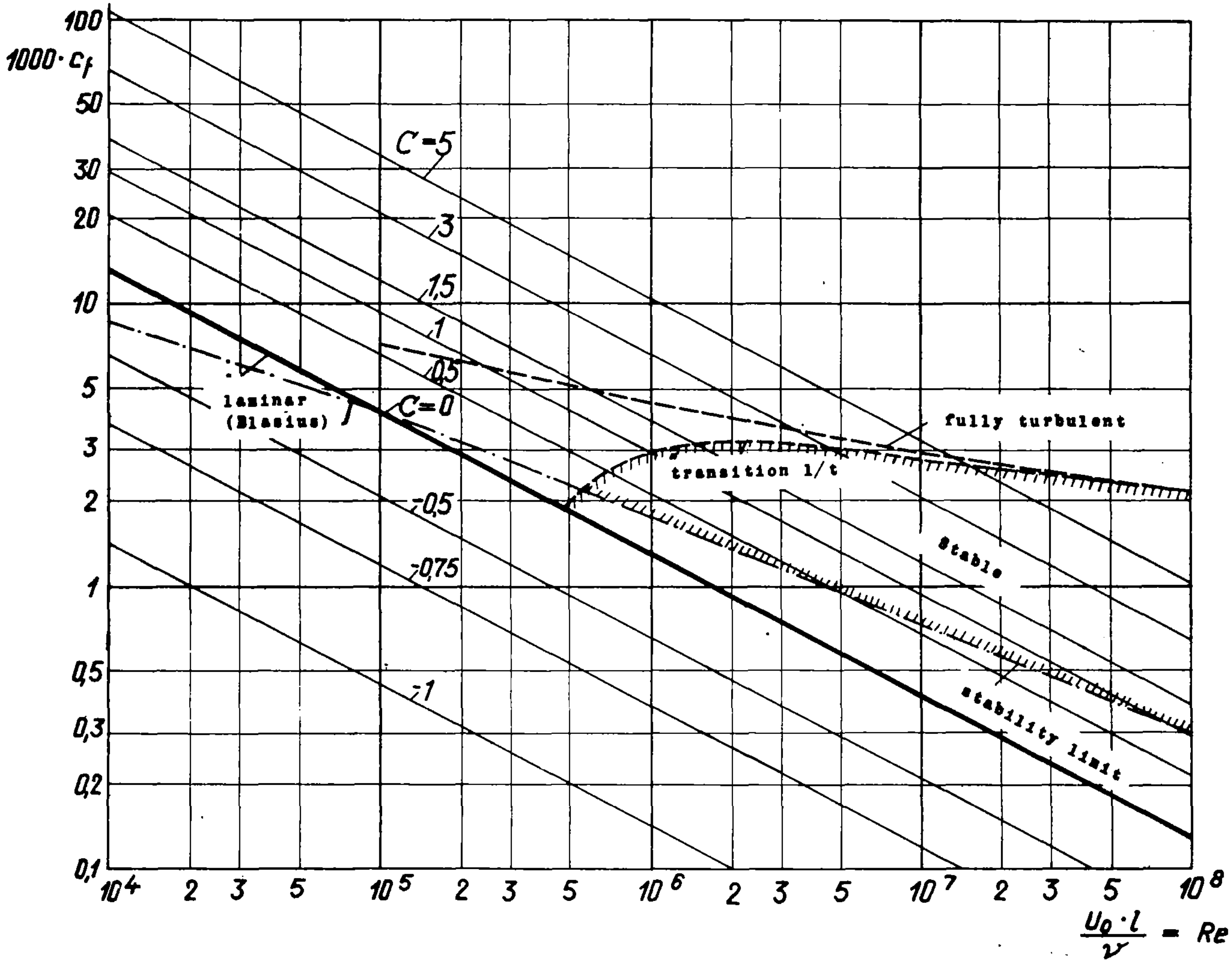

Figure 23. Drag coefficients of the flat plate with the continuous suction $v_0 \sim 1/\sqrt{x}$ and with the stability limit;

$c = c_Q \sqrt{\frac{U_0 l}{\nu}}$. $c_f = W/O \frac{\rho}{2} v^2$; O = wetted surface.

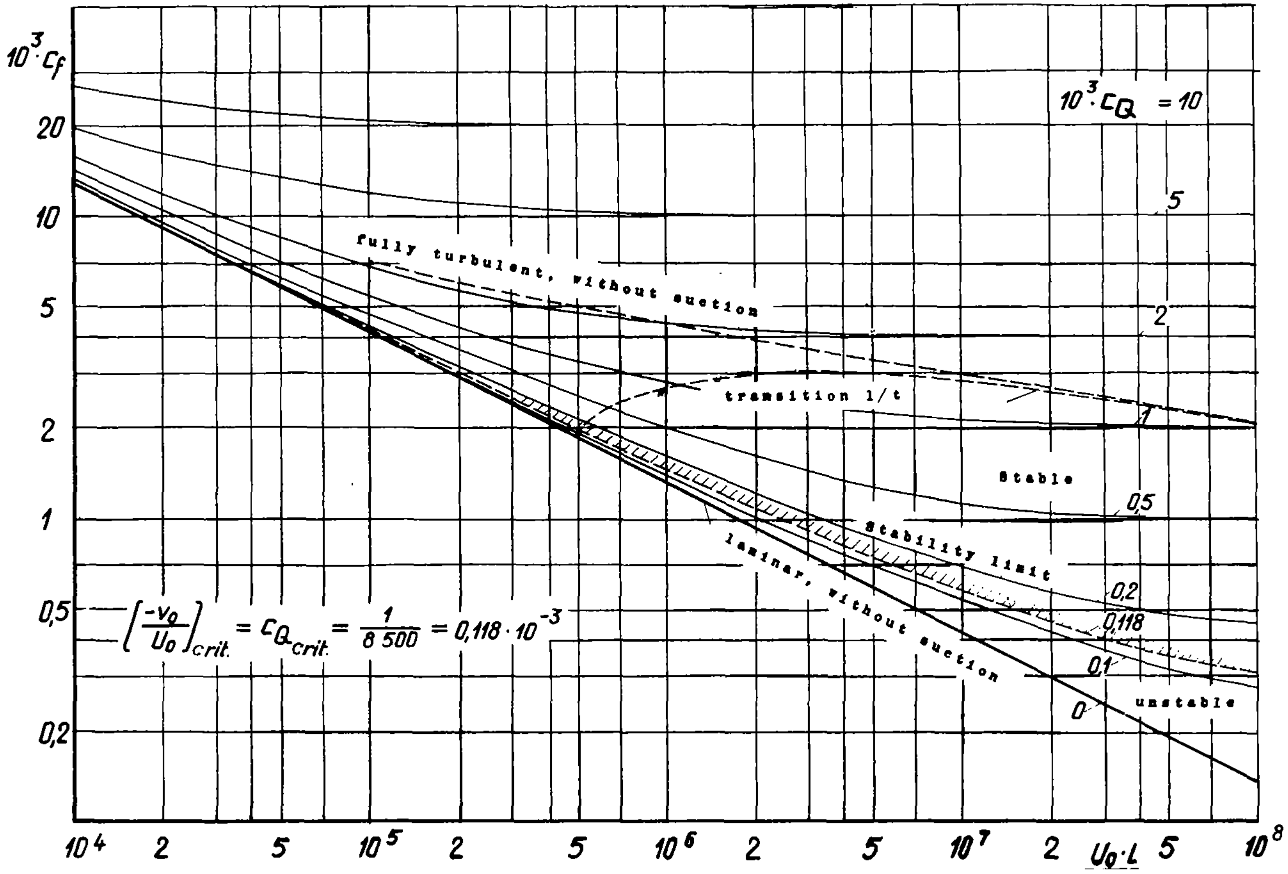

Figure 24. Drag coefficients of the flat plate with uniform suction and with the stability limit; c_f in logarithmical scale. $c_f = W/O \frac{\rho}{2} v^2$; O = wetted surface.

Laminar without suction: $c_f = 1.328 \left(\frac{U_0 l}{\nu}\right)^{-\frac{1}{2}}$ (according to Blasius).

Laminar with suction for $U_0 l/\nu \to \infty$: $c_f = 2 \frac{-v_0}{U_0} = 2\, c_Q$.

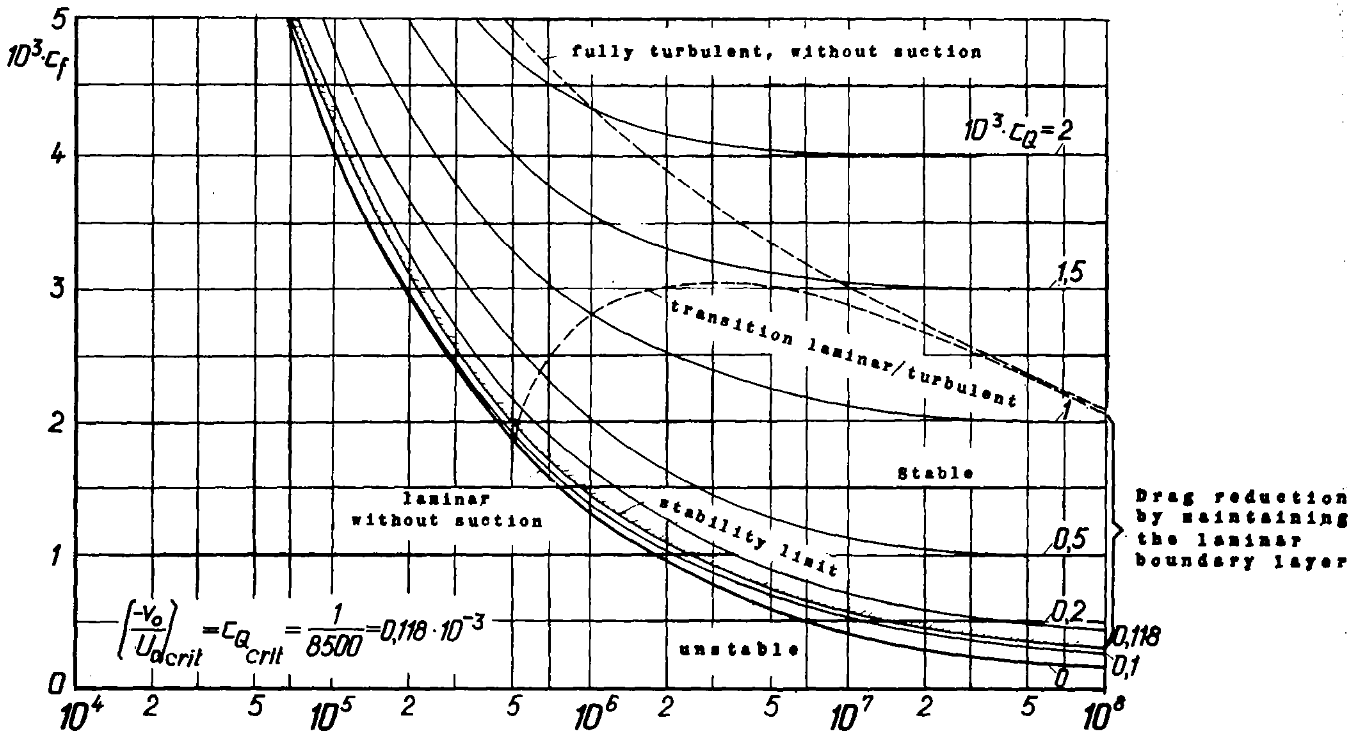

Figure 25. Drag coefficients of the flat plate with uniform suction and with the stability limit.

Laminar without suction:

$$c_f = 1.328 \left(\frac{U_0 l}{\nu}\right)^{-\frac{1}{2}} \quad \text{(according to Blasius).}$$

Laminar with suction for $U_0 l/\nu \rightarrow \infty$: $c_f = 2 \dfrac{-v_0}{U_0} = 2c_q.$

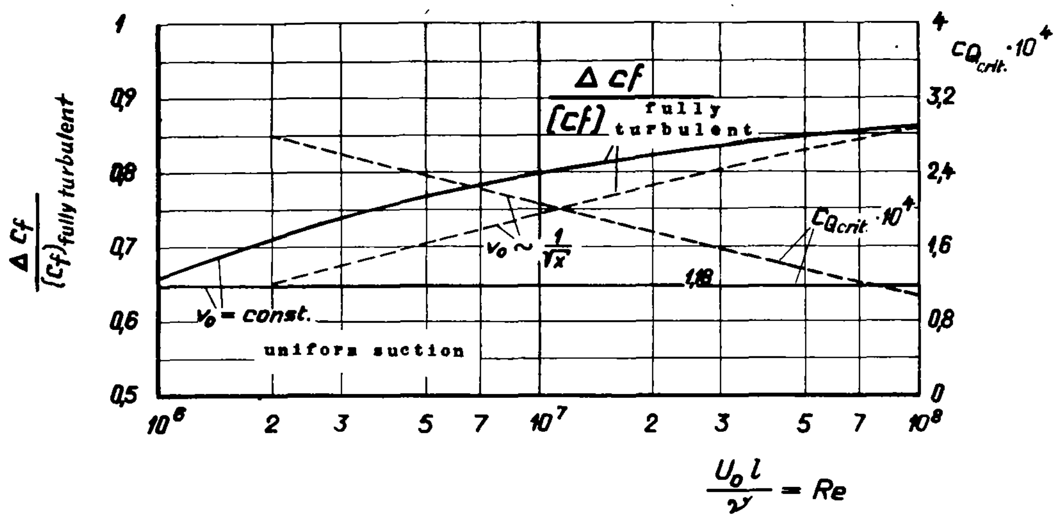

Figure 26. The relative drag reduction $\frac{\Delta c_f}{(c_f)\text{ fully turb.}}$ and the minimum suction quantity necessary for maintaining the laminar boundary layer $c_{Q\ crit}$ as a function of $Re = U_o l/\nu$ for the plate in longitudinal flow with uniform suction ($v_o \sim$ const) and with $v_o \sim 1/\sqrt{X}$. $c_f = (c_f)_{\text{fully turb.}} - (c_f)_{\text{laminar with suction}}$

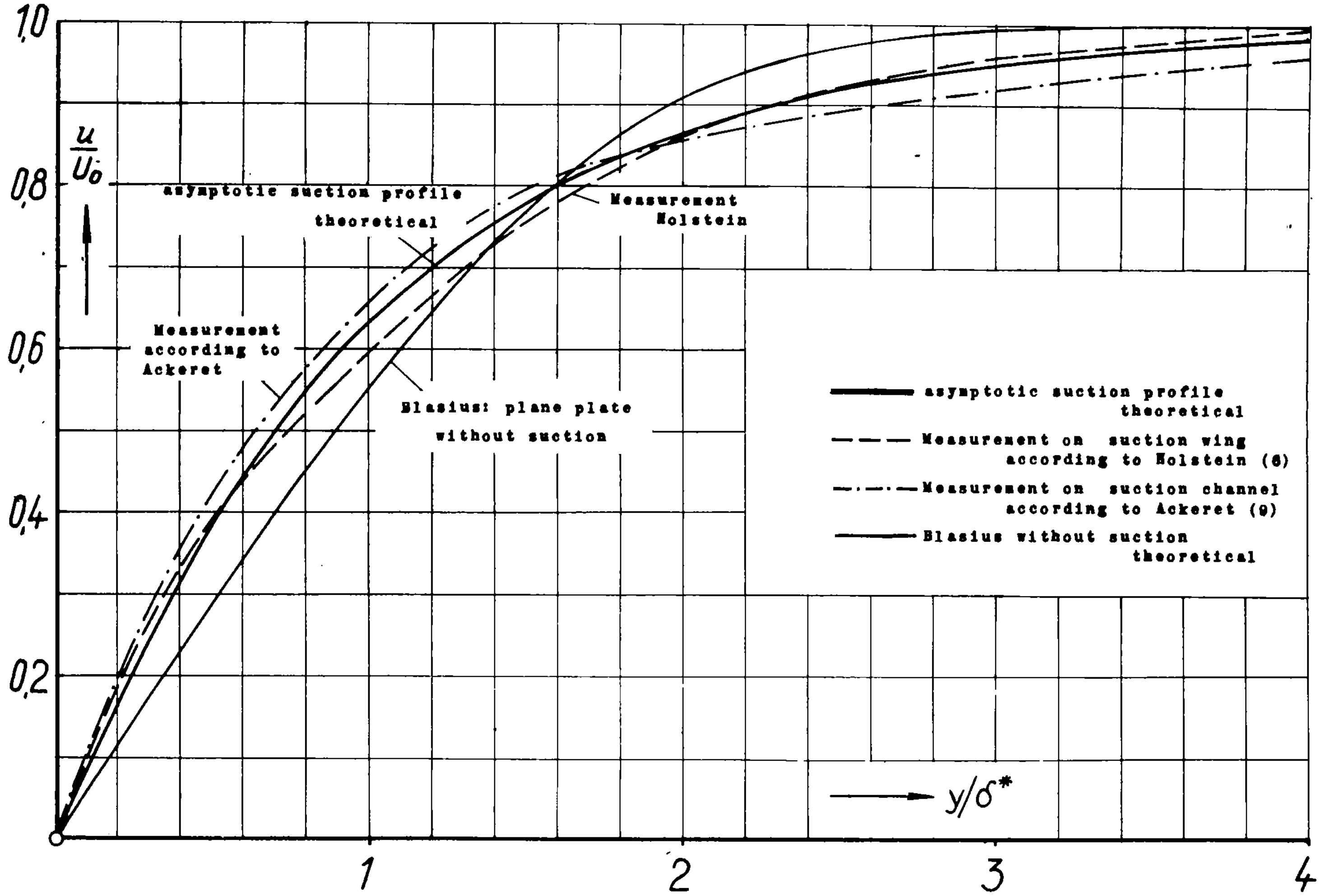

Figure 27. Comparison of the theoretical velocity distributions with the measured velocity distributions in the laminar boundary layer with suction. Displacement thickness according to Holstein [7] $\delta^* = 0.9$mm; according to Ackeret [9] $\delta^* = 0.4$mm.